Optical Measurement of Blade Edge Sharpness

A thesis

submitted in fulfilment

of the requirements for the degree

of

Master of Engineering in Electronic Engineering

at

The University of Waikato

by

Daniel Dredge

THE UNIVERSITY OF
WAIKATO
Te Whare Wānanga o Waikato

2018

Copyright

Abstract

This research aims to develop a superior way of characterizing knife sharpness. Current successful methods utilize contact destructive testing to develop a measurement protocol for sharpness however; it is in my opinion that testing in this manner, the instantaneous sharpness can never be known. Through-out this work, I investigate what physical properties determine sharpness, how failures occur in knives, the current state of art in knife sharpness testing, and then I seek to develop a new novel way of measuring knife sharpness through optical measurements.

Table of Contents

List of Figures

List of Tables

Acknowledgements

I would like to acknowledge my Supervisor Jonathan Scott, for his tremendous support through-out this research project. I would also like to acknowledge Callaghan Innovation and Anago Limited for sponsoring this work.

Dedication

Dedicated to my dear wife Tegan, and three daughters Savannah, Madelyn and Indiana. No other success can compensate for failure in the home.

Chapter 1 - Introduction

Is it possible to measure the sharpness of a knife edge non-destructively? Current commercial products measure sharpness by a physical cutting test, inadvertently dulling the knife edge in the process. This is a flawed approach. This thesis attempts to solve the question of a non-destructive measurement through developing an understanding of what physical characteristics define a sharp knife and then developing an optical based measurement approach to quantify knife sharpness.

1.1 Thesis Layout

For the research to be meaningful, and to give context for the reader, a methodical approach to the review and literature is presented in chapters 2, 3, and 4. This approach serves to introduce the reader to the current state of art in the field of knife sharpness line upon line, precept upon precept.

In the latter chapters, an approach to optically measuring sharpness is described followed by results, comparisons and conclusions.

Chapter 2 - Background

To understand the need for knife sharpness and hence the measurement thereof, it is important to know some of the basics to do with knives and their many applications. This will also be beneficial when introducing literature in later sections.

2.1 Anatomy of a Knife

There are as many types of knives and cutting instruments as there are applications, so to typify its characteristics and for simplicity of explanation, a generic commercial knife with a flat ground blade is used for a descriptive base

(Figure 1). For the purposes of this research, the majority of the knife is examined however it will be later shown that edge radius and bevel angle play critical roles in determining how sharp a blade edge is.

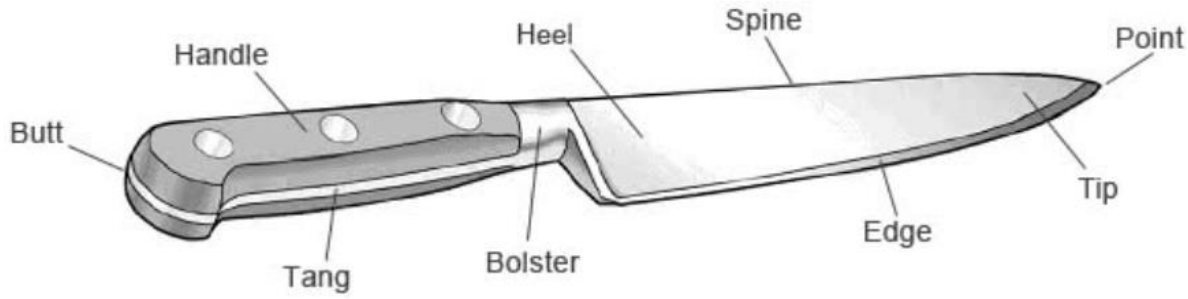

Figure 1: Graphic showing knife properties [38]

The knife mentioned above is a standard kitchen knife, forged for strength with a bolster in between the heel and the handle to provide safety for the user and overall good knife balance. The handle also known as the scales, provide a gripping surface to allow for good leverage however grip is a function of handle material.

For a long time, a wooden handle was common but of recent years, health professionals have cautioned against the use of wood due to the ability of bacteria being trapped in its surfaces. Pakkawood, a wood-plastic composite material is a common replacement which is safe to use, and gives the look and feel of real wood. Stainless steel is another common handle type which gives a very durable finish and is easy to clean, but provides very little grip when the handle becomes wet. In the meat processing industry, plastic handle knives are prevalent especially handles made in white Polypropylene. Other common types of plastics used are Fibrox, Nylon, Proflex, Resin, Styrene, Riveted Polyoxyethlene, Dexter-Russell V-Lo and Santoprene; a synthetic rubber – polypropylene composite. Each plastic composite offer small differences in comfort, grip, weight, and price.

The blade and tip have also been subject to design iterations and variations to meet the many applications in food processing (Figure 2). Generally speaking there is a trade-off between edge sharpness and edge durability. Typically, the sharper a knife edge is, the more the edge will be susceptible to rolling and cracking.

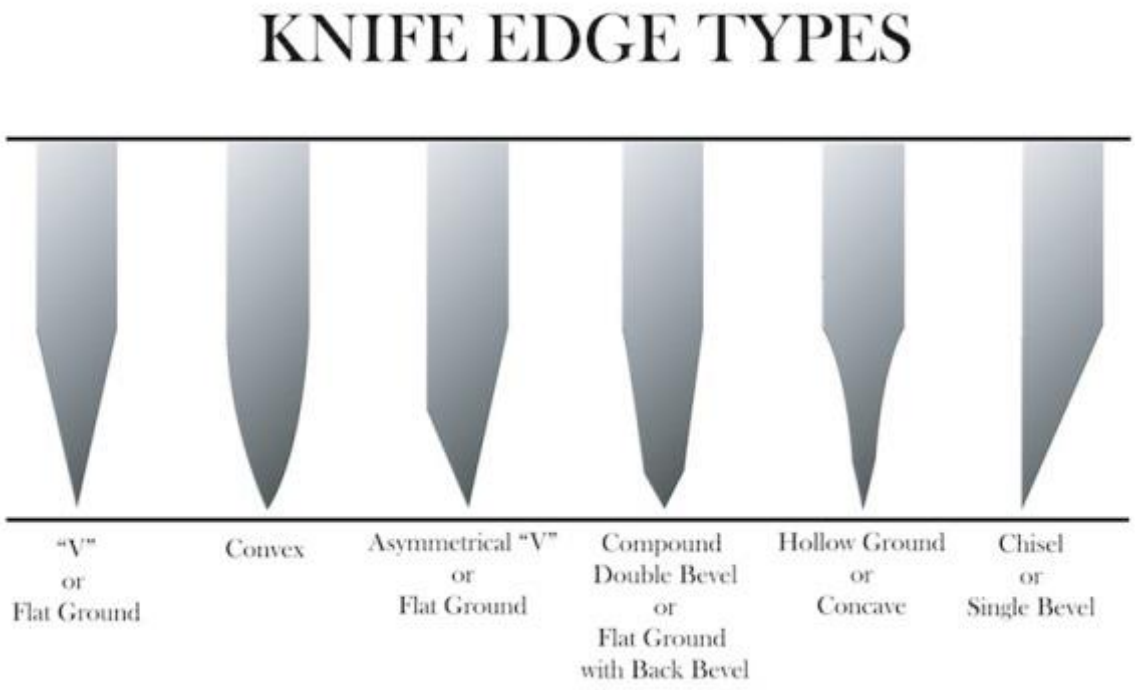

Figure 2: Graphic showing knife edge types [9]

Referring now to Figure 2, the "V" edge is the preferred design for the majority of kitchen knives as it is fairly durable and requires little skill to sharpen. The convex design is like unto the "V" but stronger due to the sloping edges allowing more steel to support the cutting edge. The hollow ground, asymmetrical "V" and the chisel are all variations trying to achieve a very sharp edge at the cost of durability. These designs all employ techniques to reduce the overall bevel angle shown in Figure 3, which, as mentioned earlier directly affects sharpness.

A typical knife used in meat cutting applications often has a double bevel angle of 40 degrees, this allows for decent levels of sharpness and durability. Other applications such as razor blades or scalpels used to cut soft solids benefit most from a double bevel angle of 15 degrees. These edges are delicate whereas in contrast, hunting knives can range from 44 to 60 degrees and are considerably more durable [33].

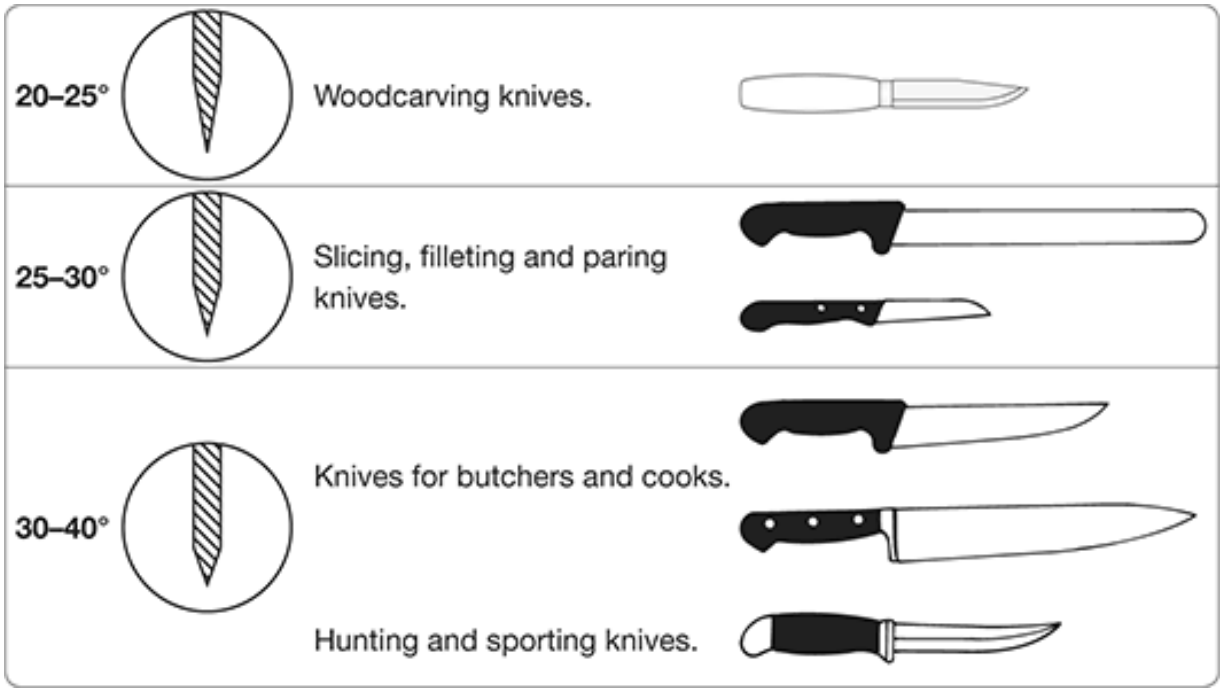

Figure 3: Graphic showing bevel angles for specific knives [36]

2.2 Knife types and Applications

In order to create a new knife sharpness test method that is broad enough to cover a range of knife designs, a review of knife types and applications is required. This is an important step in the design specification process as knives vary with application and is senseless designing a test method for every application.

Boning Knife

Boning knives, as the name implies are used to remove bones in poultry, meat, and fish. These knives have a straight edge with blade geometry for precise cuts that is curved up towards the tip which can be made stiff or flexible. They are generally 12 to 17 centimeters in length but can vary depending on culture. [38]

Bread Knife

Bread knives are used to cut bread but also sometimes used in the cutting of hard rind fruits. These knives are made with a serrated edge and are typically 17 to 25 centimeters in length [38].

Butcher Knife

The butcher's knife is an older style knife dating back to the 18^{th} century. Traditionally it was a multipurpose tool used in a range of different aspects from chopping up food and meat, to defending oneself against unbecoming behaviour. The butcher knife of today is predominantly used for cutting, sectioning and trimming large portions of meat. It features a 17 to 30 centimeter slightly curved blade, wide and heavy, ideal for cutting through large pieces of meat [38].

Chef's Knife

A chef's knife is among the most common knives used in the kitchen, because of its ability to perform a wide range of cutting tasks, such as chopping, slicing, and mincing. The knife features a 15 to 36 centimeter straight edge with a slight curve towards the tip. The chef's knife is often referred to as the "western" chef's knife as there are variants of the knife geometry in the Japanese Santoku and Gyuto knives [38].

Cimeter

The cimeter is a large curved version of the butcher's knife having a blade length of 20 to 35 centimeters, ideal for cutting and trimming steaks [10]. The term

cimeter is ancient in origins and is referenced in some religious texts often used to describe a weapon of war (Alma 43:18, Book of Mormon). Reviewing Etymology the term cimeter is a variant in spelling of scimitar, a Middle Eastern curved sword used during the Ottoman Empire [19].

Cleaver

The meat cleaver features a broad rectangular shaped blade made of soft steel predominantly used to chop through thick bone and meat. The blade edge is thick and the double bevel angle is in the range of 44 to 50 degrees. Because of the blade geometry and use, manufacturers purposely incorporate softer grades of steel so the cleaver resists chipping when chopping through coarse material [10]. The cleaver itself as a tool has origins in the Acheulean period made from stone used as a handheld axe [31].

Paring Knife

Paring knives are comparable with chef's knives as they are highly versatile in the kitchen; however they are half the size and are mainly used for cutting fruits and vegetables [38].

Scalpel

The scalpel is a small cutting instrument specifically designed for surgical applications where an extremely sharp edge is needed to penetrate human flesh or other biological materials. Historically, the great physician Hippocrates first described a surgical instrument which he called the macairion. Later, an adaptation of this early instrument by the romans called the "scallpellus" is where the modern instrument has its etymology [29]. Scalpel blades are usually made from hardened and tempered steel with a small double bevel angle of 15 degrees.

The bevel angle allows the blade to be extremely sharp, while the steel properties give increased edge durability.

The geometries examined above are in no way exhaustive by any measure; however they do provide an indicative baseline as to what is used in the kitchen and in commercial practices. To sum up this brief review, it becomes apparent that designing a test method for even this small subset of knives will be challenging. The knives described above are of various lengths, ranging from 5 to 35 centimeters, featuring curved and straight blades, and bevel angles ranging from 15 to 50 degrees; so with this amount of complexity the problem of sharpness will need to be reduced down to one or two variables in order for a testing device to be developed that can handle a broad range, and not just a select type.

This summation correlated with a definition of sharpness found in a later section will provide the necessary information to formulate a design specification.

Chapter 3 - Knife Sharpness

3.1 The Cutting Process

In every cutting process exists a material that is required to be cut which we will define as the target. The target typically then defines what cutting instrument is needed, and the process in how it is used. Quite often in other research, the authors define what the cutting process looks like for their particular application. [24] defines a sharpness testing device that simulates a deboning operation where the cutting instrument penetrates the target with the tip and then draws the instrument through the remainder of the target. The authors believe this is a representative test of cutting red meat.

[22] defines a measurement process to simulate a scalpel blade penetrating biological tissue. A scalpel blade is fixed in a device that forces the blade through polyurethane, a substitute for biological material. The authors state that this type of testing replicates the cutting action found in chopping, slicing, carving and guillotining.

In order to account for the broad range of applications a cutting instrument can be used for, a generalized model of a cutting process using a first principles approach will be reviewed. Instead of basing a measurement technique around a cutting model or technique found in industry, we will look at what is physically happening when a cutting instrument penetrates through a material.

3.1.1 Fracture Mechanics

To comprehend what is happening at the cutting surface, a small understanding of fracture mechanics is required. Fracture mechanics is the study of crack propagation in solid materials. A fracture is a crack which grows in length with

increasing applied loading stress. It is an understanding of how a crack propagates through a material and at what point the crack reaches its critical length before completely fracturing. The following equation defines the stress intensity factor, which is a value for when a crack in a material reaches the critical length [2].

$$K_C = Y\sigma\sqrt{\pi a} \quad \textbf{(3.1)}$$

Where:

K_C is the critical stress intensity factor

Y is the geometric factor (ratio of crack size to sample size)

σ is the applied stress to the material

a is the length of the crack

The critical stress intensity factor is a function of the material property, so in the case of a non-engineered material like red meat, this critical value would typically be found through testing. This value defines how tough a material is when put under a stress load, and the area under this curve on a stress-strain graph (Figure 4) defines how much energy is required to fracture said material.

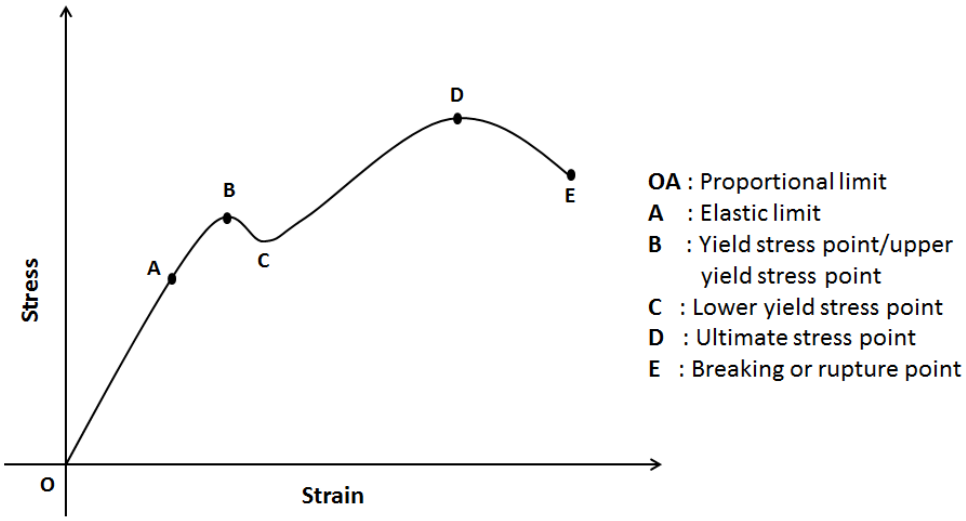

Figure 4: Graph showing points of interest for a material under loading [23]

In the study of fracture mechanics, three modes of fracture are defined (Figure 5):

- Mode I – Opening Mode, stress load applied orthogonal to material plane.
- Mode II – Shearing Mode, stress load applied in material plane.
- Mode III – Tearing Mode, stress load applied out of material plane.

In applications in food processing, each fracture mode can be represented by a given tool. The majority of cutting instruments will produce a mode I fracture; however there are cutting instruments such as carving knives or scissors that produce mode II and mode III fractures respectively. For our purposes, we examine the effects of a mode I fracture caused by indentation and penetration of a cutting instrument.

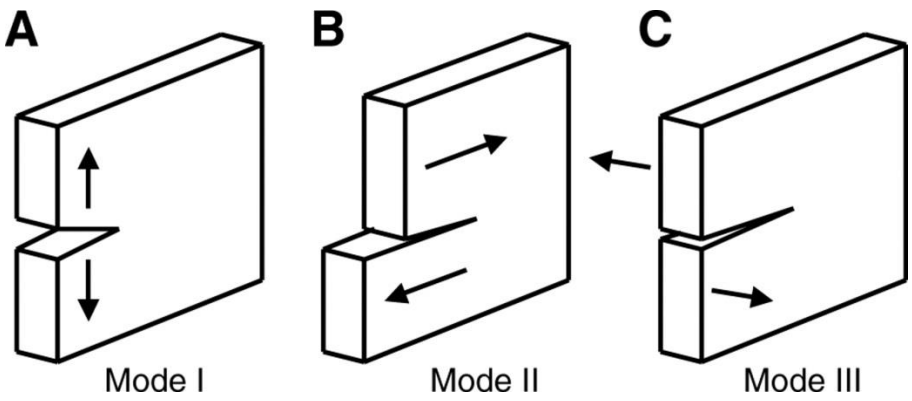

Figure 5: Graphic showing the three types of fracture modes [19]

As the instrument contacts the target, atomic bonds are broken and the crack slowly propagates under an increasing load [2].The target meanwhile exhibits an idealized elliptical shaped incision with a stress concentration factor at the crack tip defined by the following equation.

$$K_T = \frac{\sigma_{MAX}}{\sigma_0} = 2\sqrt{\frac{a}{\rho}} \qquad \textbf{(3.2)}$$

Where:

K_T is the stress concentration factor

σ_{MAX} is the maximum stress at the crack tip

σ_0 is the applied stress from the cutting device

ρ is the radius of the crack tip

a is the length of the crack

The radius of the crack tip as described by [2] is the small curvature at the peak stress point seen in Figure 6. In a study done by [21], they present a side by side geometric comparison between an experimental model, and a simulated model of a scalpel blade incision into a biomaterial. The instrument penetrates the target material inducing a mode I fracture, and it was shown that the target incision geometry reflects the cutting instrument used. Reviewing equation 3.2, it becomes clear that for the tip radius of the crack, which as just mentioned is the same radius of the edge of the cutting instrument, is critical in localizing stress to help fracture the target material. [2] points out that as the radius of the crack approaches zero, there lies an infinite stress concentration below the crack propagation. It becomes easy to see, from these deductions in fracture mechanics that cutting ability and cutting sharpness is highly correlated to the cutting edge radius.

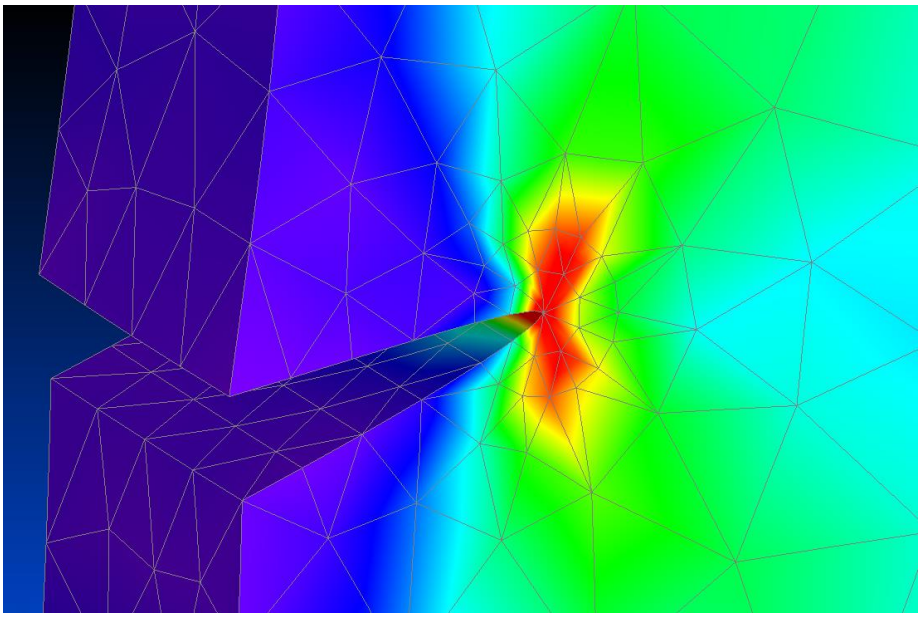

Figure 6: Graphic providing a visual representation of loading stress [23]

3.2 Failure Modes

Now that an understanding of how a cutting edge causes failure in a target material, we will now look at the physical properties of a cutting edge and determine failure modes and what failures look like. From the literature, there exist evidence of failure modes in two planes; the frontal plane (across the cutting edge) and the sagittal plane (cutting edge to spine).

The failure mode specified in the frontal plane is related to the curvature of the cutting edge. This failure is characterized by the "rolling" of the cutting edge which is evident in Figure 7. This "rolled" edge from a target perspective, sees a greater edge radius and frontal plane area than that of a straight edge. In an attempt to characterize these failure modes, high resolution images were taken of knife edges in various states of distress, using a Hitachi S-4700 cold field emission Scanning Electron Microscope (SEM). Due to the small capacity of the SEM, the blade sample size was reduced from full profile length knives, to 20mm x 10mm sub-sections. Unfortunately some of the samples became magnetized in the cutting process and hence caused drifting and resolution errors in the images. To minimize these effects, the samples were coated with both a liquid carbon ink, and plasma which increased the conductivity of the samples, and provided a greater path to the cathode.

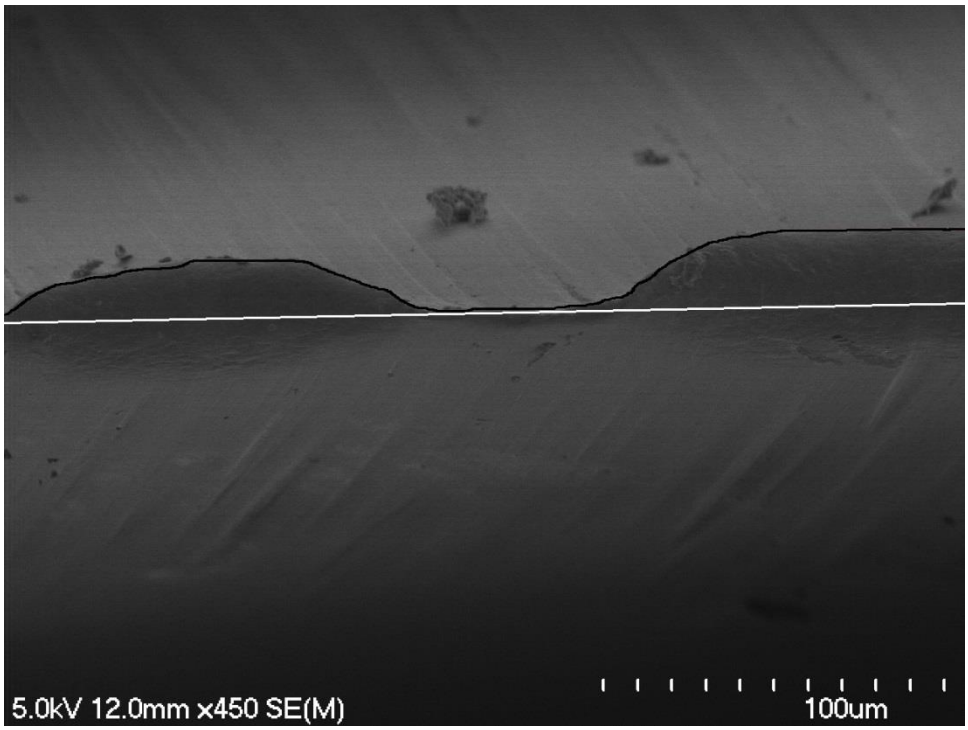

Figure 7: SEM photograph showing "rolling" on a dull edge

Referring now to Figure 7, the white line represents the true edge of the sample and the black line shows the "rolled" edge. To give a correlation between the straight edge and the "rolled" edge, the straight edge has a frontal plane width of 5 micrometers while the rolled edge ranges from 20 to 24 micrometers. Figure 8 presents a better illustration of a "rolled edge" provided by another researcher.

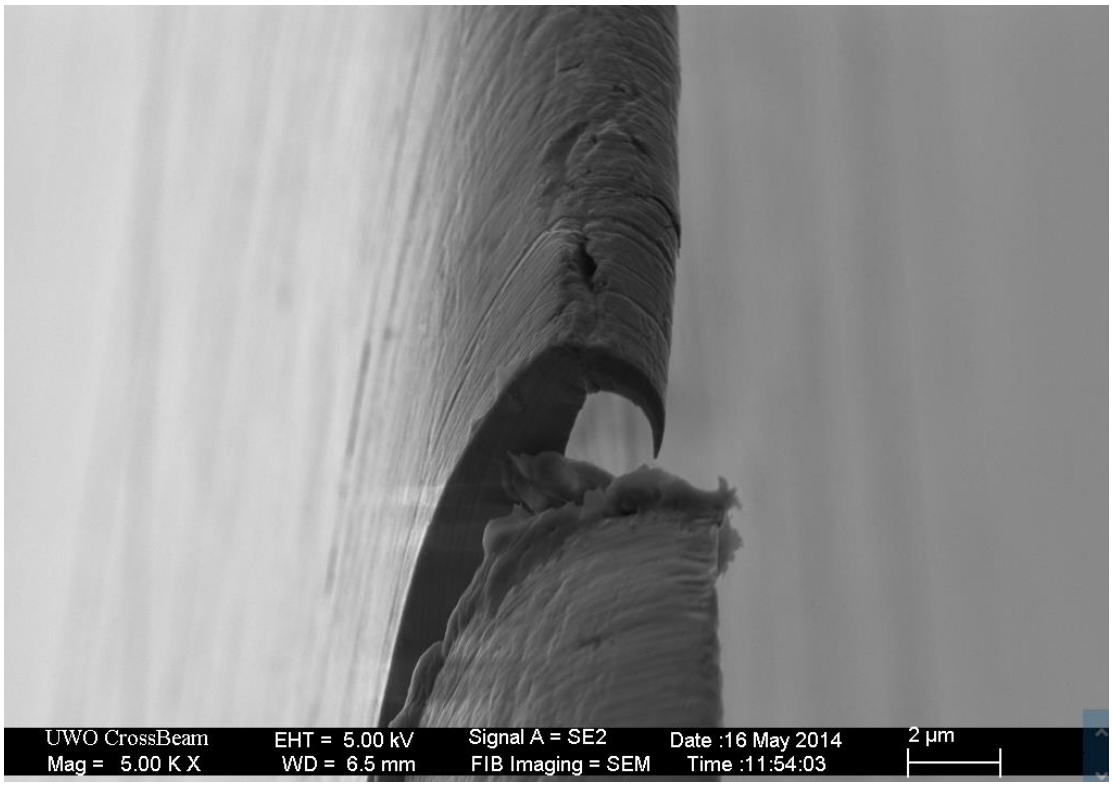

Figure 8: SEM photograph of a "rolled edge" [3]

The failure mode specified in the sagittal plane is that relating to abrasion, attrition, chipping, and fracture (Figure 9). This failure mode gives a classification to the wear experienced by a knife edge. As the depth of wear increases, the damage classification moves from light abrasion to a fracture and crack propagation. In the early stages of wear damage, the edge "rounds off" and provides an increased edge radius. In the later stages of wear damage small chips occur which lead to greater fractures. In Figure 9, [14] provides a classification for this sagittal plane failure mode; however, after reviewing SEM images collated through-out this research, it appears that this classification is in an order of magnitude too stringent.

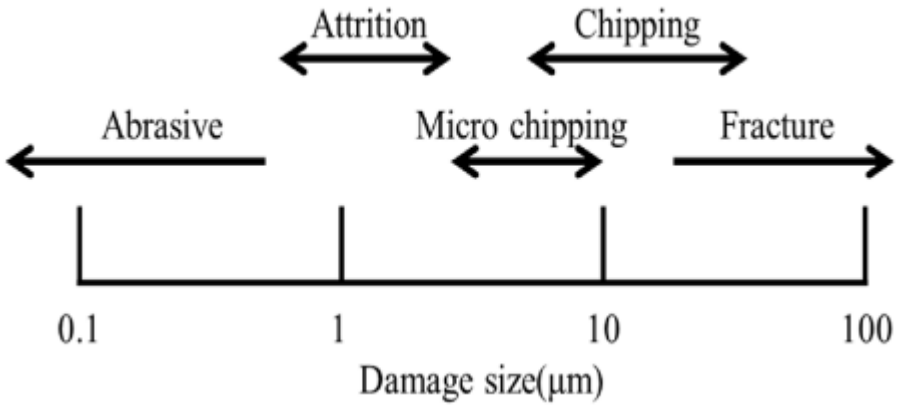

Figure 9: Graphic showing a scale for feature size failure modes [14]

3.3 Defining Sharpness

Sharpness, in a logical sense, would be the absence of the failure modes previously defined. The failure modes mentioned earlier, all point to the health of a cutting edge profile; in particularly, the edge radius. In the literature, we find that the measured applied force on a cutting instrument, as it penetrates the target material is by far the most common method of defining sharpness. However, it stands to reason that this contact destructive testing approach of defining sharpness seems counter-intuitive, as the instantaneous sharpness can never be known.

Mentioned earlier, [24] defines a sharpness testing device that simulates a deboning operation in a meat processing factory. The device measures the force along the full edge of a knife, as it is driven through a target material. The knife is then given a score based out of ten, ten theoretically would indicate that it took no force to cut the target material and that the knife edge was infinitely sharp, the opposite being true for a score of zero, being infinitely dull.

[22] defines a measurement process to simulate a scalpel blade penetrating biological tissue. A device is used to push a scalpel blade into a target material,

creating an indentation inducing modal fractures. The authors quantify a cutting metric based on the force and energy required to induce a mode I fracture, this energy being a function of the area under a curve on a stress strain graph. This metric called Blade Sharpness Index (BSI), does not discriminate locations of sharpness on a blade, but relates one sharpness value for an entire length. It is interesting to note that the authors attribute edge radius and bevel angles, citing Figures 10, 11 as determining factors in cutting sharpness, but "of the variables studied, blade sharpness was found to be most sensitive to the tip radius" [21].

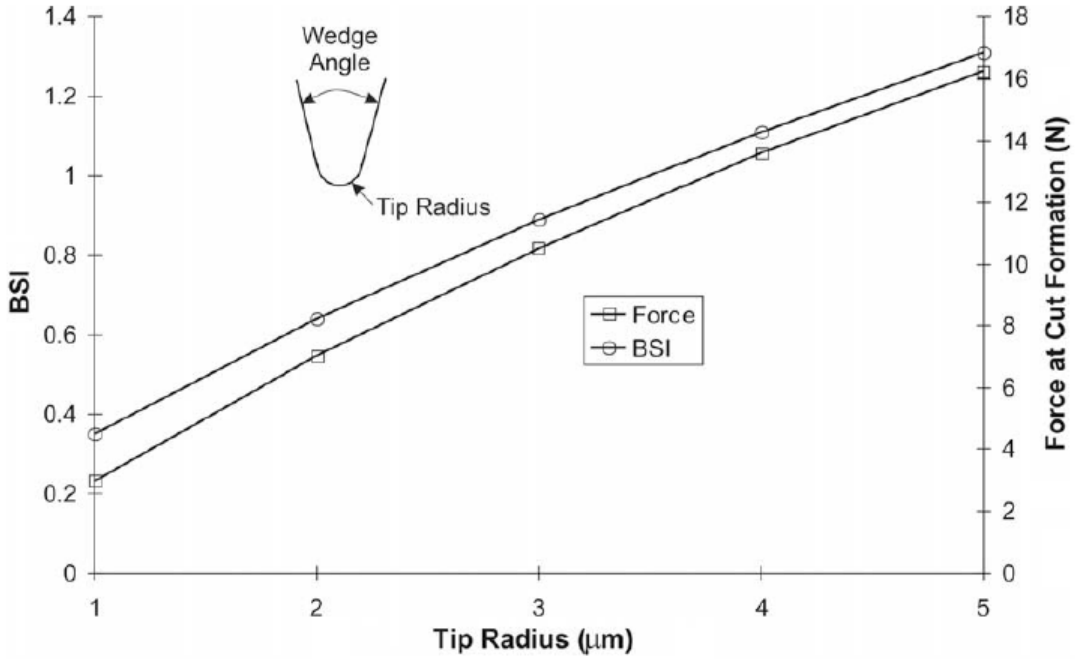

Figure 10: Graph showing the relationship between sharpness index (BSI) and edge radius (wedge angle constant at 25 degrees) [21]

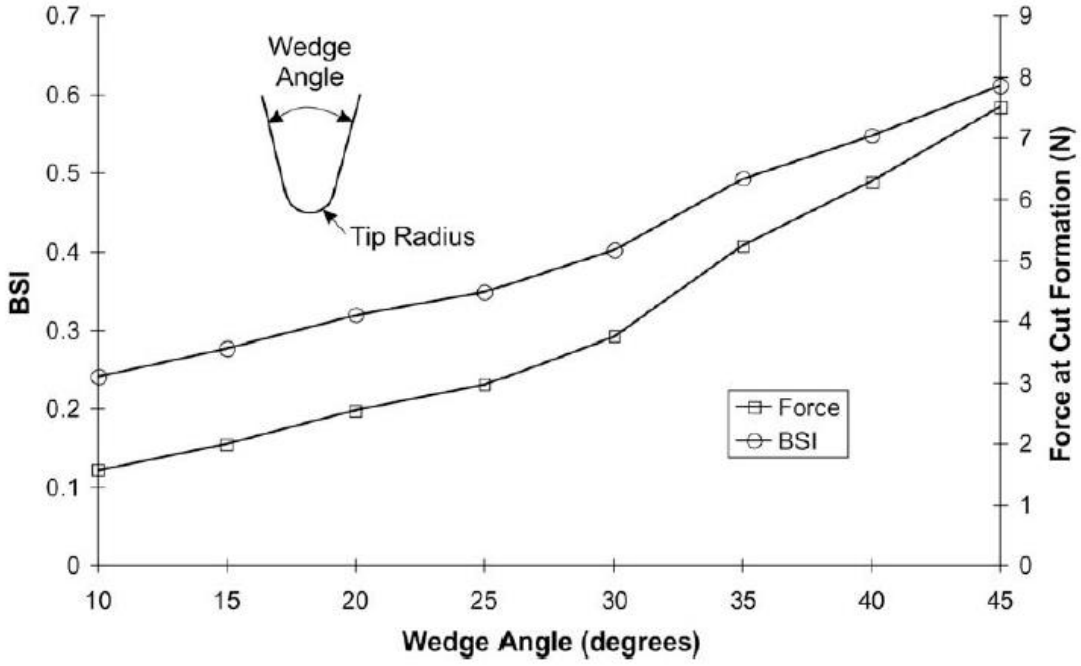

Figure 11: Graph showing the relationship between sharpness index (BSI) and wedge angle (edge radius constant at 1 micrometer) [21]

In a review of this original work by [22], [32] replicated the measuring technique to see if it could be applied to larger knives of different geometries found in the food processing industry. They concluded the technique "is suitable for characterizing the sharpness of blades for food processing", however in contrast to the original work, they found blade sharpness only depends on the cutting edge radius itself and is independent of wedge angle. Furthermore, they also discuss the idea of the technique failing when measuring materials with a more isotropic microstructure, such as cheese. Rounding off the review of force based measurement techniques; studies in the medical field were also reviewed and confirmed the relationship between force and sharpness with surgical equipment, in particularly suturing needles. [35] [37].

In the manufacturing industry, measurement techniques have been developed for tool wear monitoring. [39] performed a study on precision instruments confirming

cutting forces vary significantly with variations in the cutting edge radius. The study also confirms the theories presented in the section on fracture mechanics stating; the effect of cutting forces are linked to the localized stresses at the tool tip. In other tool wear associated research, [15] also confirms other theories regarding equation 3.2, relating the effect of the ratio of cut depth and tip radius. They state that these are important factors in tool wear, and have established that the correlation between the two is linear.

In order to visually confirm the differences between a sharp and dull knife edge, two boning knives were visually sampled using a SEM (Figure 12). Before the knives were reduced to a usable size for the SEM, each knife was put through a commercial knife sharpness testing device to confirm the levels of sharpness of each edge.

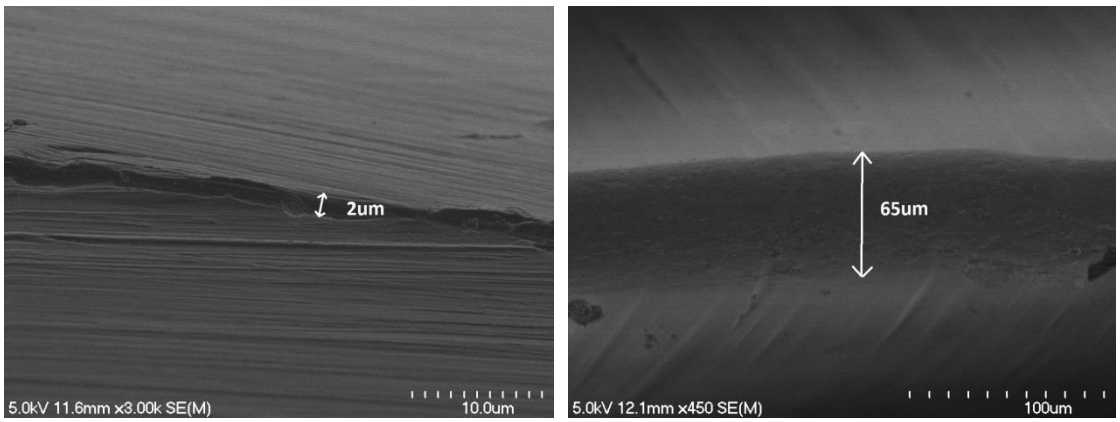

Figure 12: SEM photographs showing radii of sharp and dull edges

The comparison shows the radius of the dull edge is significantly greater, being approximately 30 times larger. From equation 3.2, the sharper edge would produce four times the amount of stress concentration compared with the dull edge; significantly increasing the ability to cut the material.

3.4 The Effect of Knife Sharpness

3.4.1 Health and Safety

The cutting edge profile has great impact on grip forces and cutting moments experienced by professional meat cutters. [25] performed field tests and observed correlations between knife sharpness and cutting performance concluding an increased knife sharpness yields reductions in cutting times, mean cutting moments, and in mean and peak grip force. In a later review by [34] lists repetition, speed, force and posture are key risk factors for musculoskeletal disorders in the meat processing industry, knife sharpness being a critical sub-factor. [25] suggests with improved knife sharpness, the cutting times would allow meat processing staff longer or more frequent "micro-breaks". These breaks could then serve as a time to maintain knives or to recuperate from repetitive and awkward postures imposed by meat cutting techniques.

3.4.2 Fruits and Vegetables

Knife sharpness also impacts the quality of fresh cut fruit and vegetables. As an injury response mechanism due to being cut, fresh fruit and vegetables exhibit an abiotic stress potential that significantly impacts the quality of the freshly cut produce. A dull knife increases this stress potential which exhibits greater "discoloration (e.g. browning of fresh-cut surfaces), increased respiration and ethylene evolution, loss of flavour and texture, weight loss, decline in levels of ascorbate, development of off-odours, membrane breakdown, and tissue softening" as observed by [13].

Chapter 4 - Current State of Art

4.1 Contact Measurement Methods

4.1.1 Anago Knife Sharpness Tester

Anago has a range of knife sharpness testing devices that are specifically designed for the medical and meat processing industries. The inventor attributes industry health and safety as motivation for creating these devices [24]. The original device patented in 2005, emulates a cutting motion that is common in meat cutting processes, such that the target material being cut is penetrated by the knife tip first, and followed by the full blade edge; the knife being situated in a cradle on a 45 degree slope (Figure 13). The target material is a polypropylene-coated fiberglass rectangular mesh with a grating size of 1.0mm x 1.7mm and a strand thickness of 0.8mm.

Figure 13: Graphic of the Anago knife sharpness tester [1]

As the knife is brought through the target material, a load cell measures the amount of force used to cut each strand. While a linear potentiometer tracks the

position of the knife, the cutting force is sampled by an analog to digital converter at a sampling rate of 100 Hz. As the knife moves down the 45 degree decline, the full knife length is sampled.

Based on an idealized micro-scale model (Figure 14) of the measuring process, the following assumptions are made:

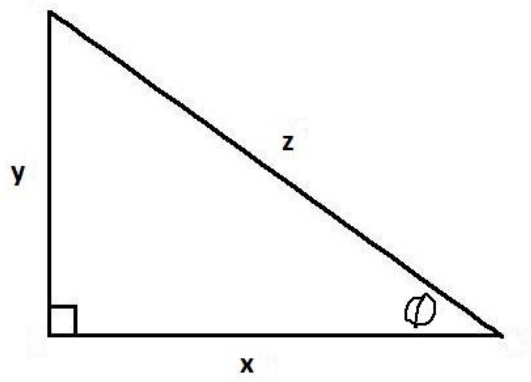

Figure 14: Diagram of idealized model of Anago measuring device

$$x = y \tan \emptyset \quad \textbf{(4.1)}$$

$$z = \sqrt{x^2 + y^2} \quad \textbf{(4.2)}$$

Where:

$\emptyset = 45°$ (declination angle)

$y = 1.7\ mm + 0.8\ mm$ (mesh length + strand depth)

x is the knife edge resolution

z is the lateral knife movement

Resolving equation 4.1 and 4.2, we find the idealized measurement resolution to be 2.5 mm and a lateral knife movement of 3.5 mm. With a sample rate of 100 Hz and a cutting speed in the z direction of 40 mm/s, oscillations should be apparent in the output data, reaching minimum force with singular or no strand cuts and peak forces when the knife cuts through more than one strand (because of knife

curvature) with a period of 2.5 mm. Figure 15 shows the raw data taken from a knife sharpness test with a knife receiving an 8.5/10 score.

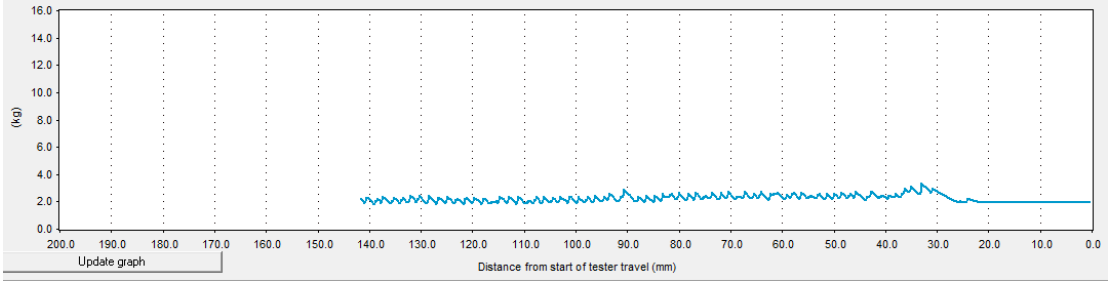

Figure 15: Graph of raw data from Anago measuring device showing oscillations

Reviewing the data of Figure 15, it was found that the period of oscillation was on average 1.9 mm. The 2.5 mm value was based on an idealized model of a straight knife with no curve; however, factoring in the curvature of a standard boning knife this could make up the discrepancy between the calculated and measured values.

Referring now to the target material used with this product, the company employs an ingenious method to help alleviate crack propagation by using a mesh based material. Based on their internal research, the fracture properties of this material are highly comparable to red meat having a mean correlation coefficient of 0.89; this does call into question their claim of this method being non-destructive, unless red meat itself doesn't cause wear to the cutting edge which is unlikely. Perhaps if a knife was only tested once in this device, the resulting wear would be negligible, however, after performing more than 100 knife tests with this device, it was necessary to test a knife more than once in order to get an accurate reading. The variance between tests on a single knife can have an average difference of 5-10% with spots along the knife reaching 30%. The variance is far more dramatic

with dull knifes than with sharp knives. Figures 16 and 17 provide illustrations of the variance in data for a knife with an average score of 5.68 and 8.69 respectively

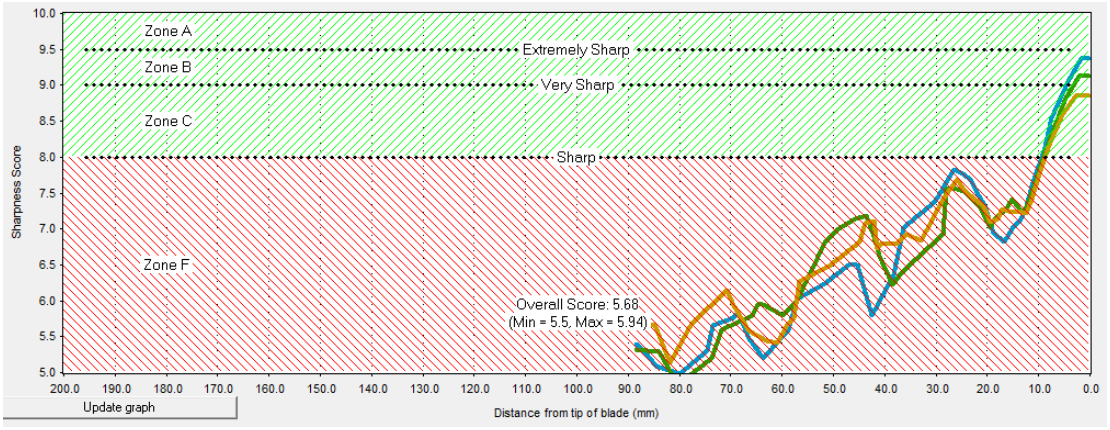

Figure 16: Graph from Anago measuring device showing sharpness levels of a dull knife

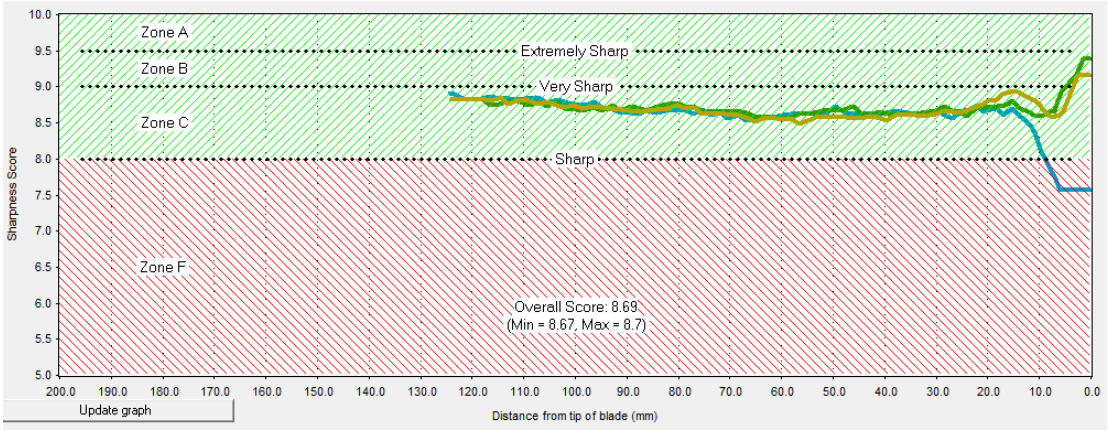

Figure 17: Graph from Anago measuring device showing sharpness levels of a sharp knife

It is important to note that these knives performed these tests back to back without being used in between, as such it can be concluded at lower sharpness levels, the data becomes noisy.

Overall the Anago KST is perfect for the food processing industry, as it can supply the industry with knowledge of a full knife profile, and use that data for sharpening and training purposes.

4.1.2 CATRA sharpness tester

CATRA (Cutlery & Allied Trades Research Association) have two styles of sharpness testing machines, one performs sharpness and life tests (Figure 18) while the other is only a sharpness tester for smaller blades (Figure 19). The life tester uses impregnated synthetic paper as a target material which is lowered onto the cutting edge and oscillated back and forth while the depth of cut is recorded. This is repeated two more times and the sum of the three cuts give the cutting index for the knife tested. Figure 18 presents sample data from this CATRA life tester [5].

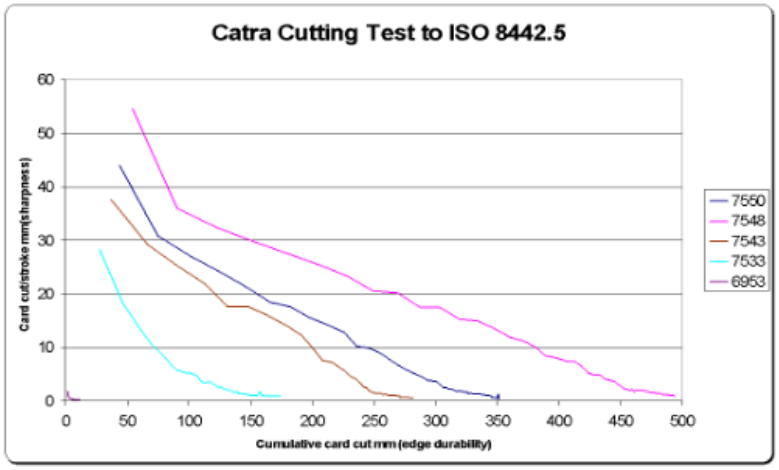

Figure 18: Graph from CATRA life tester showing results from four knives [5]

As mentioned, the sum of the first three cuts determines knife sharpness, while the other cuts show how the knife fairs over cumulative cuts and thus is a measure of life. CATRA provide a baseline index in which a knife must meet a certain depth of cut to be at a specific sharpness level.

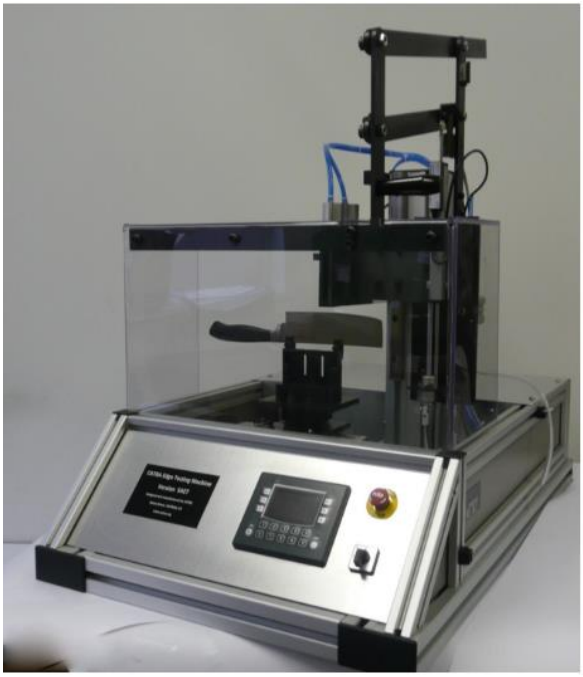

Figure 19: Graphic showing the CATRA life testing machine [5]

The second machine mentioned illustrated in Figure 20, is a smaller sharpness testing machine which is based on the constant cut depth method. This testing technique pushes the knife edge into the target material silicon rubber, and a load cell captures the force data. This data is then compared with the following index supplied by CATRA [6].

Blade Type	Typical Sharpness Levels (N)
Razor Blade	0.3 to 0.4
Scalpel Blade	0.4 to 0.6
Utility Razor Blade	1.0 to 1.4
Kitchen Knife	1.8 to 3
Hunting Knife	1.9 to 3.5
Well Worn Blade	6.0 to 11.0

Table 1 Force thresholds to determine sharpness for each knife type

A couple of critiques about these CATRA measuring machines, both are destructive testing methods, with the life testing machine dulling the blade until it cuts no more. Both machines also present data for only a portion of the cutting edge profile which is not representable for the entire length.

Figure 20: Graphic showing the CATRA sharpness testing machine [6]

4.1.3 Haida International Equipment

The knife sharpness performance test machine is like unto the CATRA life tester. The machine uses a petroleum resin based synthetic paper as a target material and the accumulative cut depth achieved is the sharpness level [12].

4.1.4 Edge on up

Edge on up have developed a series of small measuring instruments capable of measuring the sharpness levels of razor blades and common kitchen knives (Figure 21). The small profile of the device appears to be made for a household kitchen. Edge on up employ a force based sharpness approach by measuring the force it takes the knife to cut through a thin piece of string. This measurement is

localized to a single point on the knife edge no more than the width of the string. The testing method appears simple, however it is fairly subjective. The force applied to the knife edge is manually controlled by the user and not by a repeatable system. [4] [7]

Figure 21: Graphic of edge on up testing device [7]

4.2 Non-Contact Measurement Methods

4.2.1 Optical interferometry

[14] describes a tool wear monitoring technique using interferometry, which classifies tool damage into two categories, abrasion, and attrition. The technique uses a 5mW 633 nm laser diode to illuminate the tool surface and an avalanche photodiode as a receiver. The authors define the term knife edge interferometry, carefully denoting the differences between their interferometry technique, and the main stream Michelson interferometry, but as it stands to reason the interferometry they are defining, is clearly diffraction (Figure 22).

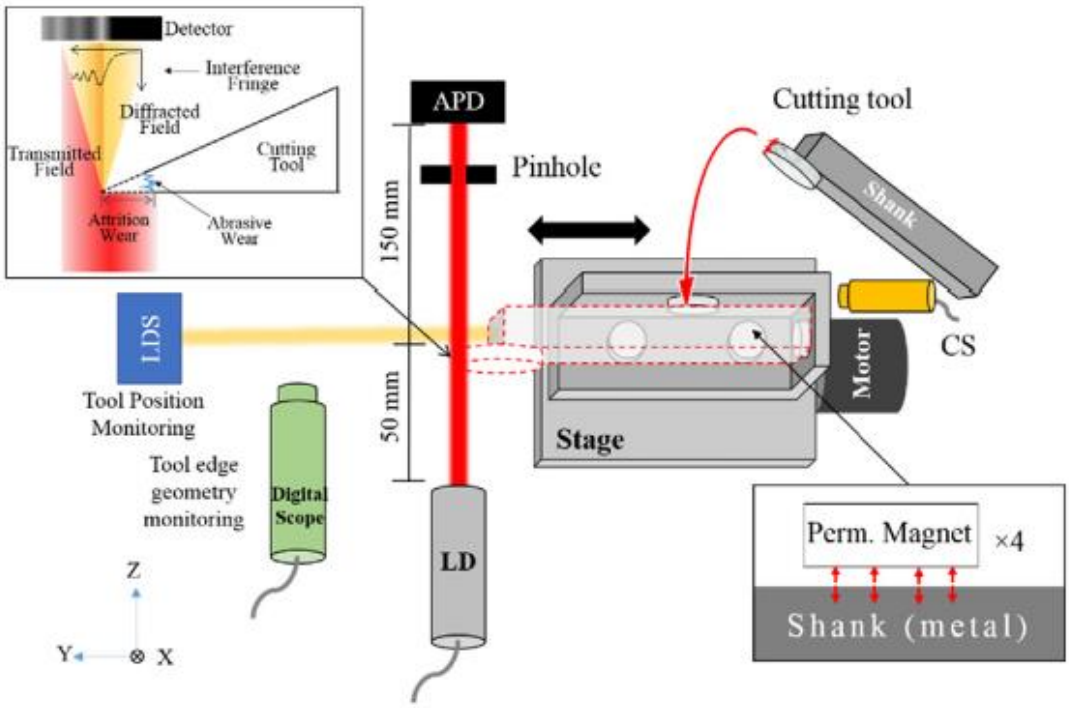

Figure 22: Diagram of the knife edge interferometry device [14]

The authors characterize tool wear by measuring the fringes of the diffracted light in the transmitted field of the diffraction pattern. They attribute a measured phase shift (Figure 23) as evidence between a new tool and a tool with 1 – 5 micrometers of edge reduction.

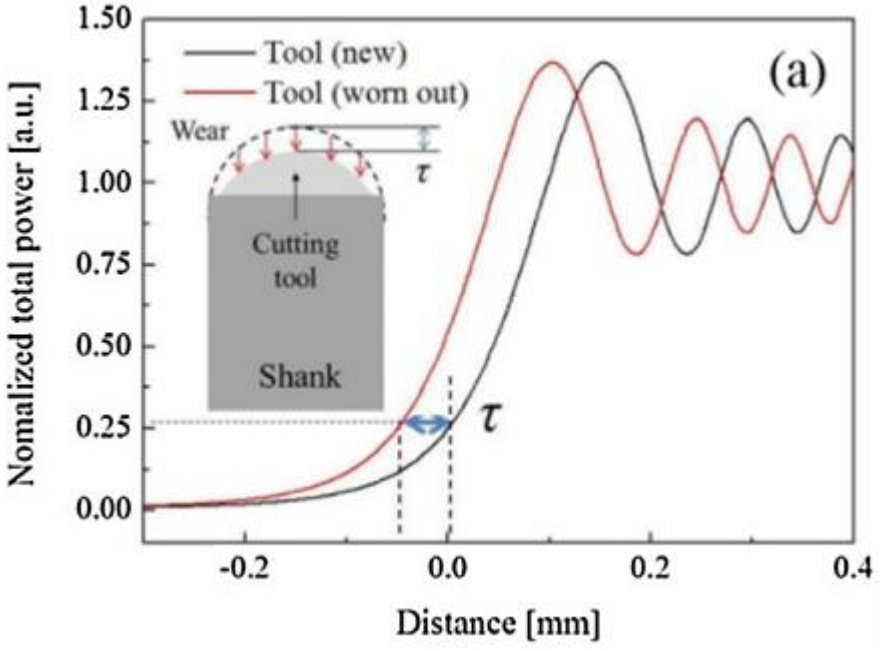

Figure 23: Graph showing attrition represented by a phase shift [14]

The authors attribute signal attenuation to very fine abrasive wear ranging from less than 0.1 – 1 micrometers of damage (Figure 24). Although the authors of this test method are not directly characterizing sharpness, but are measuring surface roughness; it is fascinating to see the resolution capabilities of using a fine light source to resolve sub-micrometer detail [14]. Other studies also show how diffraction is a useful measurement technique to resolve displacement [8] [17].

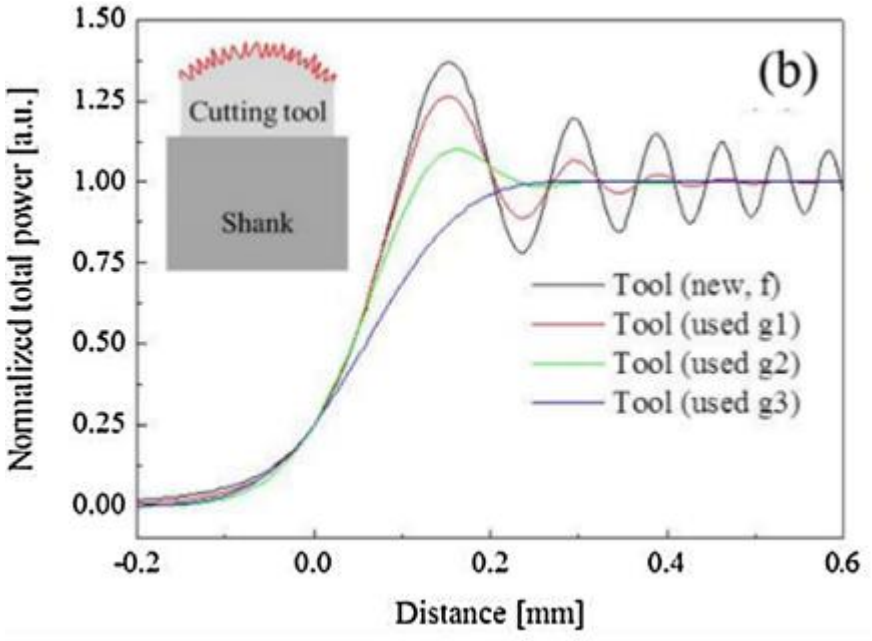

Figure 24: Graph showing abrasion represented by signal attenuation [14]

4.2.2 Optical sharpness meter

The optical sharpness meter is a device that measures and quantifies the degree of sharpness along a blade. Light is directed at the sharpened edge and a measure is taken of the intensity of reflected light. The reflected light varies with sharpness (Figure 25). Robert, the inventor believes that the duller the blade, the greater the radius of the blade will be, therefore more surface area for light to be reflected [16].

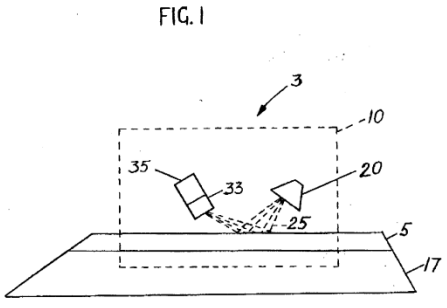

Figure 25: Diagram of the sharpness meter [16]

An interesting beginning point in this research was to experimentally reproduce this sharpness meter in a lab setting. Figure 26 shows a dulled boning knife under

a light microscope. It is interesting to see how easy it is tell if the knife was dull and at which moments along the blade were affected, due to the reflected light because of the increase in radius.

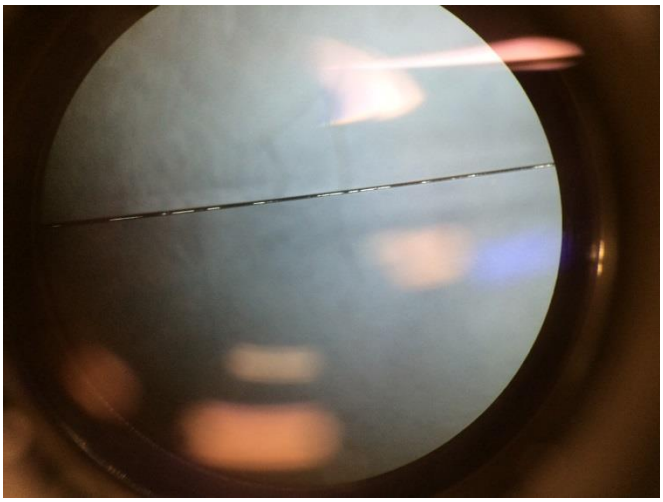

Figure 26: Photograph showing experimental results of light reflection study

4.3 Conclusions

Only the most relevant findings were reported in this section as there were a host of other measuring devices reviewed, however most had the same fundamental measurement technique. Of the technologies presented in this section, Anago's knife sharpness tester is by far the most complete measurement technique on the market today. Although a great product, the Anago knife sharpness tester can be improved on; appearing to be an opening in the market for a high quality, non-contact, high resolution sharpness tester.

Chapter 5 - Design of Measurement Device

5.2 Design Specification

A culmination of the research presented in this thesis, drives the design specification process in designing a new measurement technique and device. Table 2 presents the specification.

Specification	**Description**
Measuring Variable	Cutting edge radius (edge width)
Target Material	NA
Measuring Capability	Full profile, tip to heel, left and right bevels. 0.1 to 200 micrometer damage size.
Contact Type	Non-contact
Testing Type	Non-destructive
Size	Small manual version, larger automated version, suitable for house hold kitchen use.

Table 2 Design specification

5.3 Concept

To meet the needs of the design specification, an optical based prototype will be conceptually produced and verified. In relation to work performed by [14], we will describe an optical diffraction measurement technique for the quantifying of sharpness through a frontal plane radius measurement; parting from, and separate to the work performed by [14].

Diffraction is defined as the bending of light around obstacles into its geometrical shadow (Figure 27). The founding principles of diffraction come from the wave nature of light, formally called Huygens' theory, after Christiaan Huygens.

Huygens' stated that "Each point on a wave front acts as a source of secondary wavelets, the combination of these secondary wavelets produces the new wave front in the direction of propagation" [40]. Diffraction, as applied in electromagnetic wave theory, aptly termed the Knife-edge effect, gives estimations about path loses when electromagnetic waves come in contact with objects, such as hills and mountain peaks. When an obstruction is introduced between a transmitter and a receiver, the transmitting signal is required to run a longer path length in order to complete the transmission (Figure 28). This additional path can incur signal attenuation or diffraction losses depending on the complexity of the obstacle. Any additional losses are added to the total transmission loss.

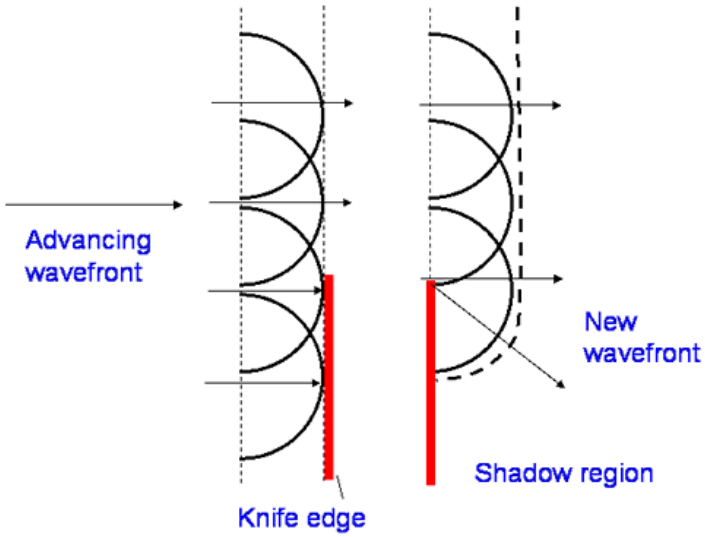

Figure 27: Graphic showing wave fronts interacting with knife edge underpinning Huygens principle of light propagation [40]

In order to understand the mechanics of signal loss, a discussion including formulae will be used to establish an understanding of diffraction attenuation about basic shapes. If we recall the basic model of diffraction loss which is based on a knife edge (Figure 28), the additional path length as shown can be summarized by the following equation:

$$\Delta d = h^2 \frac{d_1 + d_2}{2 d_1 d_2} \quad \textbf{(5.1)}$$

Where:

Δd is path length difference

h is the height of the obstacle above the line of sight reference

d_1 and d_2 are the distances from the transmitter to the obstacle and from the obstacle to the receiver respectively.

From equation 5.1 we observe that the path length difference is a squared relationship with obstacle height, therefore, to reduce path loss; a reduction in obstacle height above the line of sight reference is required.

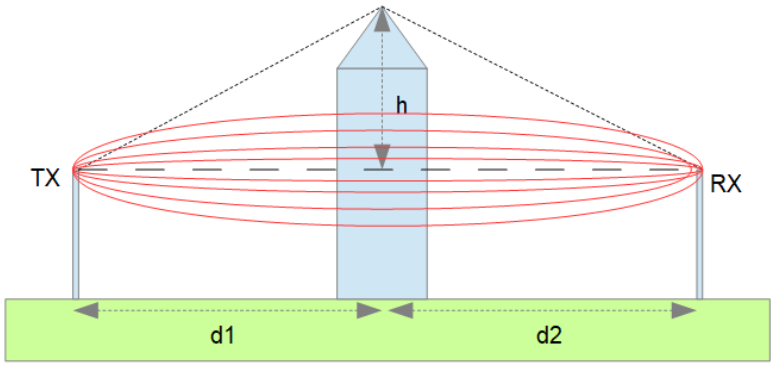

Figure 28: Diagram showing a model of a sharp knife edge with a new path with a height denoted by h and Fresnel zones in red.

An increase in path length difference can also be attributed to the shape of the obstacle. Figure 29 illustrates a dull knife edge with the signal running a tangential path along the radius of the top surface; this not only increases the overall path length difference but also causes loss due to the interaction of the signal with the surface of the obstacle producing tangential attenuation [26].

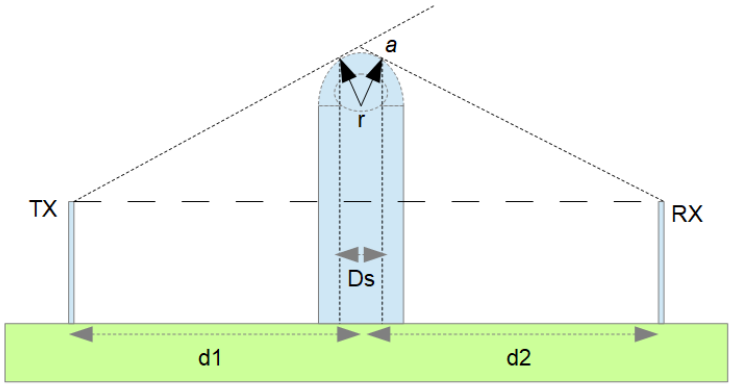

Figure 29: Diagram showing a model of a dull knife edge with a new path with a radius denoted by r and the transmitted angle denoted by α.

Tangential attenuation is the excess loss incurred by the signal contacting the surface of the obstacle and is defined as [11]:

$$L_{ex} = 11.7\alpha \times \sqrt{\frac{\pi r}{\lambda}} \quad \textbf{(5.2)}$$

Where:

L_{ex} is the excess loss due to the tangential path

α is the angle of the path in radians

r is the radius of the obstacle

λ is the wavelength of the signal

To find the total loss by the diffracted path, we add the excess loss to the solution to the Complex Fresnel Integral, $F(v)$. A good approximation for this integral is described by the following equation [26].

$$F(v) = 6.9 + 20\log\sqrt{(v-0.1)^2 + 1 + v - 0.1} \qquad v \geq -0.7 \quad \textbf{(5.3)}$$

Where:

v is the Fresnel-Kirchhoff parameter which relates path length difference and wavelength shown by the following:

$$v = 2\sqrt{\frac{|\Delta d|}{\lambda}} \quad \textbf{(5.4)}$$

Where:

$|\Delta d|$ is the path length difference from line of sight

λ is the wavelength of the transmitted signal

We find that if the path length difference $|\Delta d|$ equals zero, this is known as "grazing path" and the solution to the Fresnel Integral equals ~ 6dB, so even just coming in contact with the surface of an obstacle degrades the signal by one half (Figure 30). This segues into a related concept mentioned previously and illustrated in Figure 28, Fresnel zones are a good way to maintain signal quality using ½ wavelengths as boundary conditions. They are related to path length difference with each zone an integer multiple of a ½ wavelength. For odd integer multiples, the multipath interference from the diffracted signal is destructive, whilst even multiples produce constructive interference.

For this purpose, industry uses a rule of thumb for microwave links of a minimum 60% of the first Fresnel zone to remain clear of obstacles [40]. To calculate the amount of phase shift related to the Fresnel zone for a given path length difference is defined by the following equation [26]:

$$\theta = \frac{\pi}{2}v^2 \quad \textbf{(5.5)}$$

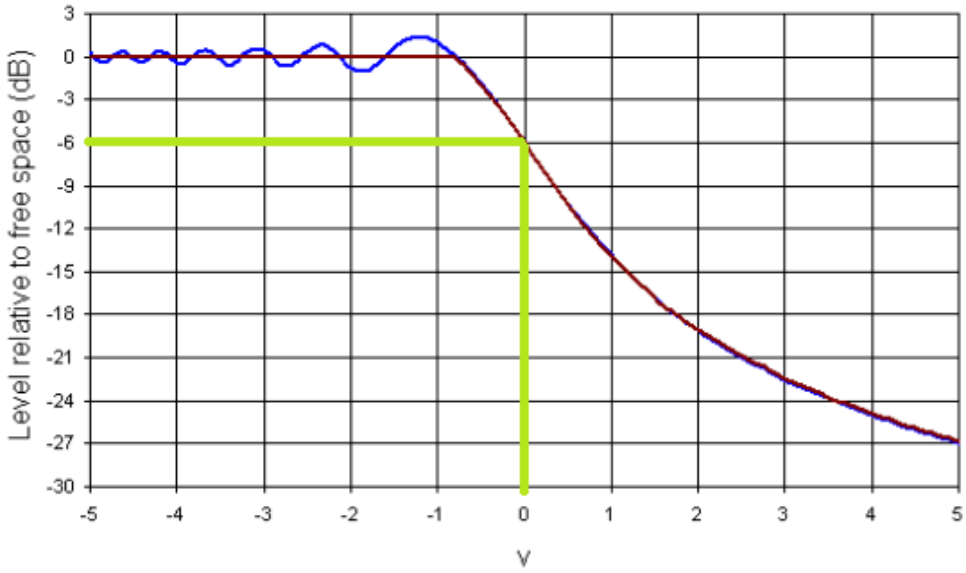

Figure 30: Graph illustrating Equation 5.3 showing at v=0 ("Grazing path") the signal loss equals 6 dB

Reverting back to knife sharpness and the measurement of edge radius, we will define our measurement technique as the amount of signal intensity at a given measurement angle and attempt to establish a relationship between knife edge radius and signal intensity. The parameters for the proof of concept design will be set as follows:

- The offset angle α at which the intensity measurement will be taken is 7 degrees. This specific angle was chosen to match the halfway point on our test prototype measuring system cable of measure from 0 – 14 degrees, 0 degrees being grazing path.
- The height h at which the knife edge will protrude into the laser beam will be 0.26mm, being approximately half of the Gaussian beam diameter.
- The laser will be located 0.1 meters from the knife sample
- The receiver will be located 0.23 meters from the knife sample

From these parameters we can deduce the following:

$$\Delta \boldsymbol{d} = (0.00026m)^2 \frac{0.1m + 0.23m}{2 \times 0.1m \times 0.23m} = \mathbf{485\ nm} \quad \textbf{(5.6)}$$

$$\boldsymbol{v} = 2\sqrt{\frac{485\ nm}{633\ nm}} = \mathbf{1.75} \quad \textbf{(5.7)}$$

$$\boldsymbol{F(v)} = 6.9 + 20\log\sqrt{(1.77 - 0.1)^2 + 1} + 1.77 - 0.1 \quad \textbf{(5.8)}$$

$$= \mathbf{14.22\ dB}$$

$$\boldsymbol{\theta} = \frac{\pi}{2}1.77^2 = \mathbf{282\ degrees} \quad \textbf{(5.9)}$$

$$\therefore 360 - 282 = \mathbf{78\ degree\ phase\ lag}$$

$$\boldsymbol{L_{ex}(sharp\ knife)} = 11.7 \times 0.1222\sqrt{\frac{\pi \times 500nm}{633nm}} \quad \textbf{(5.10)}$$

$$= \mathbf{2.25\ dB}$$

$$\boldsymbol{L_{ex}(dull\ knife)} = 11.7 \times 0.1222\sqrt{\frac{\pi \times 50000nm}{633nm}} \quad \textbf{(5.11)}$$

$$= \mathbf{22.52\ dB}$$

From equations 5.6 – 5.11 we can theoretically predict a difference in path length of 485 nm with a multipath phase lag of 78 degrees giving constructive interference with a 1.56 times increase in gain. Neglecting any changes in path difference that might arise from a dull edge we calculate a diffraction loss of 14.22 dB. The tangential excess loss calculated at a 7-degree offset will give a range of 2 – 22 dB depending on the sharpness of the knife edge.

These calculations are only indicative as there will be other factors at play including measurement noise, errors in test setup, and other light interference.

The measurement technique will be validated through cross-correlation of the data from a proof of concept prototype, the Anago knife tester, and SEM images. The

equations introduced in this section will be later used to verify and clarify the results obtained.

5.4 Proof of Concept Design

5.4.1 Concept Validation Design

In order to carry out a proof of concept, a completely new test set up was required to be developed. The test set up required a monochromatic point source, a knife sample holder on a linear translation stage, and an optical receiver on a rotational stage (Figure 31). Early iterations of this proof of concept design involved the use of an optical chopper and lock in amplifier. This was removed in the later stages as testing was performed in a dark room providing very little noise on the receiver.

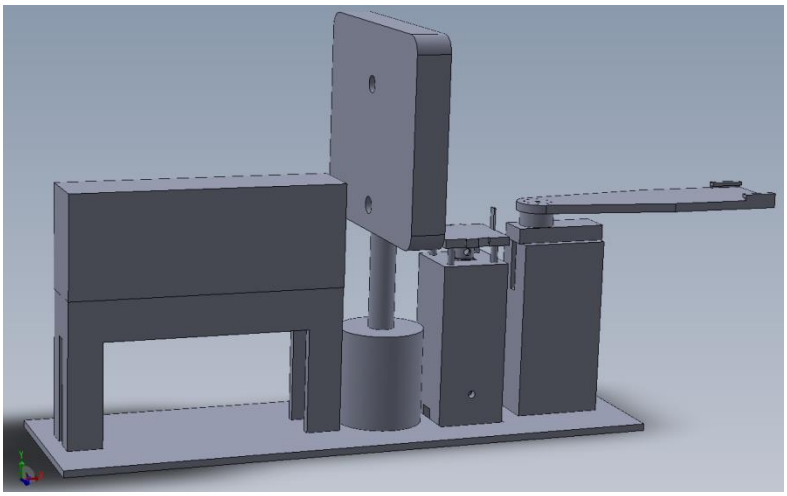

Figure 31: Graphic showing experimental test set up model

5.4.2 Light Source

The light source selected was a 1mW 633 nm He Ne laser placed atop of a stand (Figure 32). The distance from the laser to the knife sample was carefully considered as this has repercussions on sample resolution and Gaussian beam intensity. A few experiments were carried out to obtain the beam waist radius as

no documentation was available for our particular laser. The distance from the laser to the sample was decided by the following calculations:

$$z_0 = \frac{\pi {w_0}^2}{\lambda} \tag{5.12}$$

$$w(z) = w_0 \sqrt{1 + \left(\frac{z}{z_0}\right)^2} \tag{5.13}$$

Where:

z_0 is the Rayleigh range

w_0 = 0.25 mm (beam waist radius)

λ = 633 nm

$w(z)$ is the beam radius at an arbitrary point z

Resolving equation 5.12, we find a maximum Rayleigh range of 0.31 meters. A distance of 0.1 meters was chosen for the distance between the laser and the sample as to keep the sample within the Rayleigh range, allowing maximum beam intensity, little to no divergence and a beam radius no bigger than $w(z) \times \sqrt{2}$. To get an exact beam radius projected onto the knife edge, we resolve equation 5.13 and find the beam diameter to be 0.525 mm.

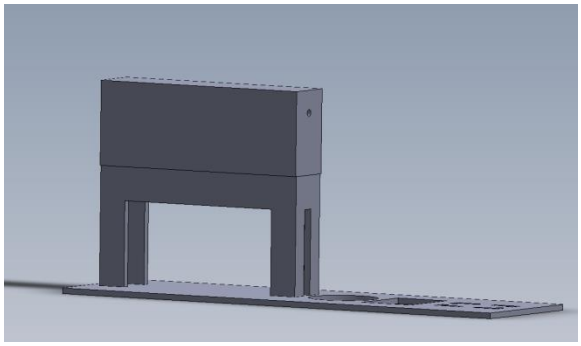

Figure 32: Graphic showing laser and stand module

5.4.4 Sample Holder Translation Stage

A translation stage was built underneath the sample holder, which allowed for a precise height adjustment (Figure 33). It was driven by a small Actuonix linear actuator with a motion range of 30 mm and a minimum step of 1 mm.

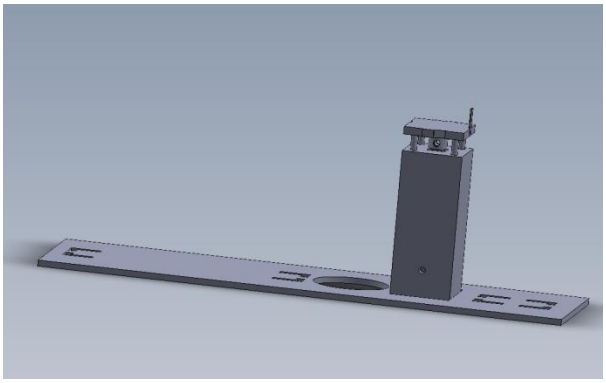

Figure 33: Graphic showing the sample translation stage module

5.4.5 Receiver Rotational Translation Stage

The receiver was placed at the end of a swing arm coupled to a servo motor. This meant each data point collected would be located at the same radius as the rest of the data, making the data more comparable (Figure 34). It is noted however, there is a small offset between the sample and point of rotation. This does not affect the data in any way, as it is a constant seen by all data points.

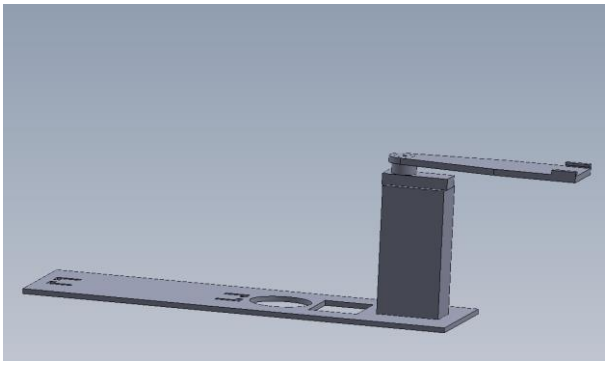

Figure 34: Graphic showing the receiver module

5.4.6 Signal and Data Acquisition

The signal data was captured by a photo diode and amplified through a trans-impedance amplifier. This data was then sampled by an analog to digital converter with 12 bits of resolution and stored on a PC.

Chapter 6 - Instrument Tests and Verification

6.1 Instrument Tests

To confirm the validity of the diffraction measurement theory, three independent boning knives were brought to three different sharpness levels through a wearing process. Each knife was then tested in the Anago knife sharpness testing machine, giving each knife a score out of ten. We will define these knives as A, B, and C with respective sharpness scores of 8.5, 6.5, and 5.5.

Once the knives were formally tested, each knife was cut down to small 20 mm x 10 mm segments, being very careful not to ruin the cutting edge. Once cut, the knife samples were examined and photographed in microscopic resolution to ascertain each knives respective edge radius.

After scrupulously imaging each segment, the samples were then measured using the new diffraction proof of concept prototype. One segment from each knife A, B, and C which showed best correlation to their Anago sharpness value were measured. The prototype device then took ten successive measurements in 1 mm increments along the cutting edge. For each increment, three measurements were taken so the data could be averaged to reduce the effects of noise in the system. In total 1200 data points were obtained to classify these samples. Once the data had been collated, the average was taken of the three datasets for each of the ten tests and the gain was calculated using equation 6.1

$$dB = 20 \log \frac{v_2}{v_1} \tag{6.1}$$

Where:

v_2 is the measured diffracted signal intensity after subtracting background light.

v_1 is the maximum measured un-diffracted signal intensity after subtracting background light.

Figures 35, 36, and 37 show the data obtained from knives A (8.5), B (6.5), and C (5.5) respectively. To reiterate, the method of measuring sharpness as found in the previous chapter, we measured the intensity of the received light at a 7 degree offset angle. The value measured will be indicative of the knife sharpness at that location on the blade.

The data has been manipulated to show the correlation between edge feature size and gain measurement. The data has been illustrated in this way to show how signal intensity varies with edge radius proving the validity of this measurement technique.

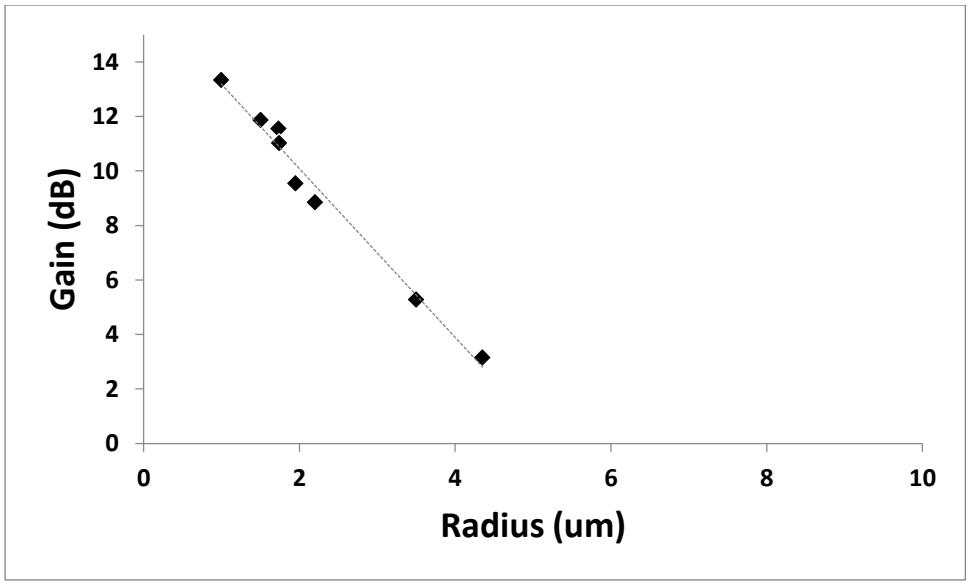

Figure 35: Graph showing the results from sample A (KST 8.5).

In Figure 35, we find that the data is situated within a 4-micron area which was expected for a knife with a KST score of 8.5; being reasonably uniformly sharp. The gain associated with these measurements also appears to decrease linearly with increasing radius; noting a 10-dB difference between a 1 micron radius edge and a 5 micron radius edge.

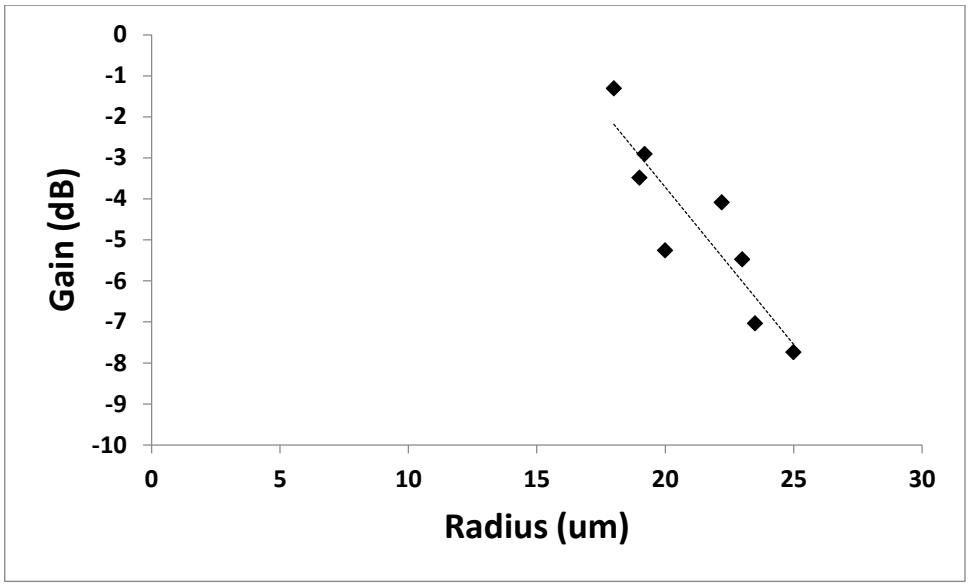

Figure 36: Graph showing the results from sample B (KST 6.5)

In Figure 36 we find again a small spread in the measured values spanning 5 microns. This knife sample appears uniformly dull unlike that of the knife sample presented in Figure 37. In the below Figure we find quite a wide spread in sharpness values. This is what would typically be expected as a knife with a KST score of 5.5 isn't uniformly dull but has sections of sharp and dull spots along the length of the blade. This was confirmed early on in the research by observing a dull knife under a light microscope as shown in Figure 26.

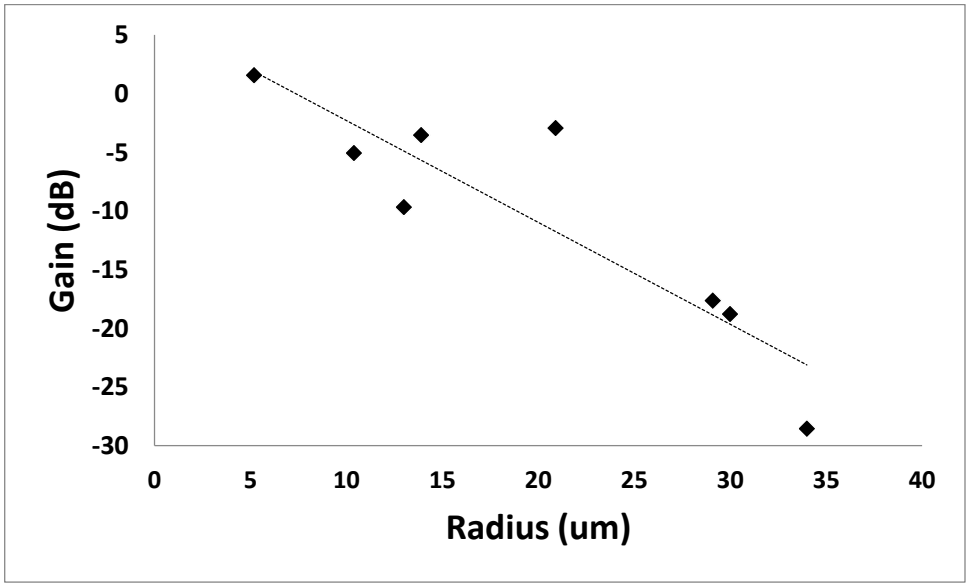

Figure 37: Graph showing the results from sample C (KST 5.5).

Below in figure 38, we see the relationship between each knife sample set showing a general linear decrease with increasing radius which is a great result for this research, as this is what was expected. A sharp knife will diffract more light than a duller a knife which is what we can see from the below figure

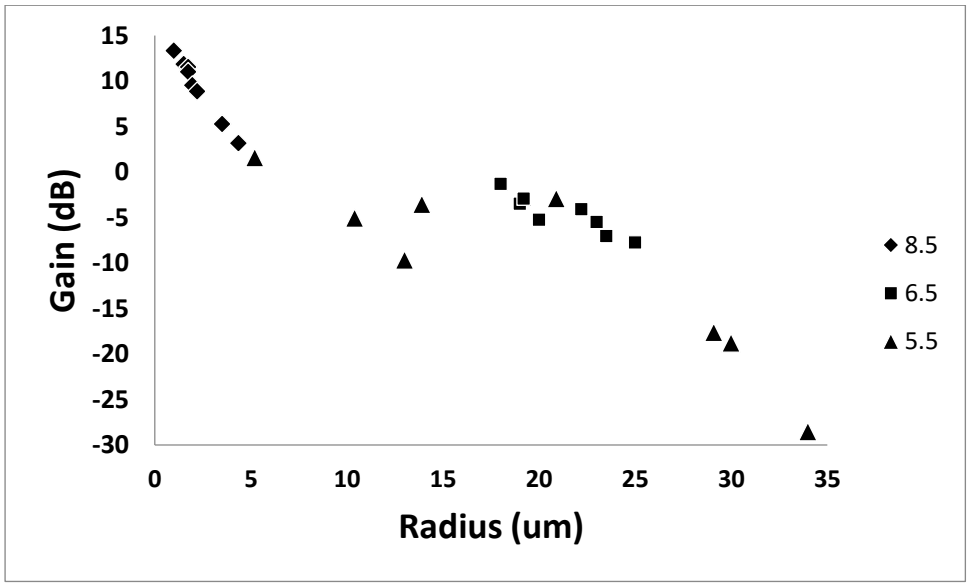

Figure 38: Graph showing a comparison of feature size to diffracted light between knife samples

We note the small gradient differences between the data of each sample, this could be due to the sample positioning on the rotational stage causing a small offset error. As an aside, referring to [14], the authors mention attrition wear is characterized by a phase shift in the data. When setting the sample on the stage, we notice the position was critical to minimize any additional variances in the data caused by a phase shift. The small offset error mentioned earlier could be a result of this.

We see that the sharper 8.5 blade has a stronger correlation with a linear trend compared with the duller 5.5 blade. This could be in part due to the measurement technique of the SEM. An image is captured at 1mm increments with each image

spanning about 70µm of the blade edge. This capture size would only allow for about 7% of the knife to be imaged which would be inadequate for duller edges, as variance would occur in the other 90% of the 1mm sections (Figure 44). This could be addressed in future work.

Returning to the assumptions formulated in chapter 5.

1. We note from Equations 5.6 to 5.11 that a 14 dB diffraction loss is estimated based on a path length difference of half a Gaussian distribution.
2. We expected gain from the constructive interference given by the theoretical 78 degree phase shift between the obstructed and un-obstructed beam (Figure 39).
3. We also expected excess loss due to the interaction with the surface of the knife at offset angles.

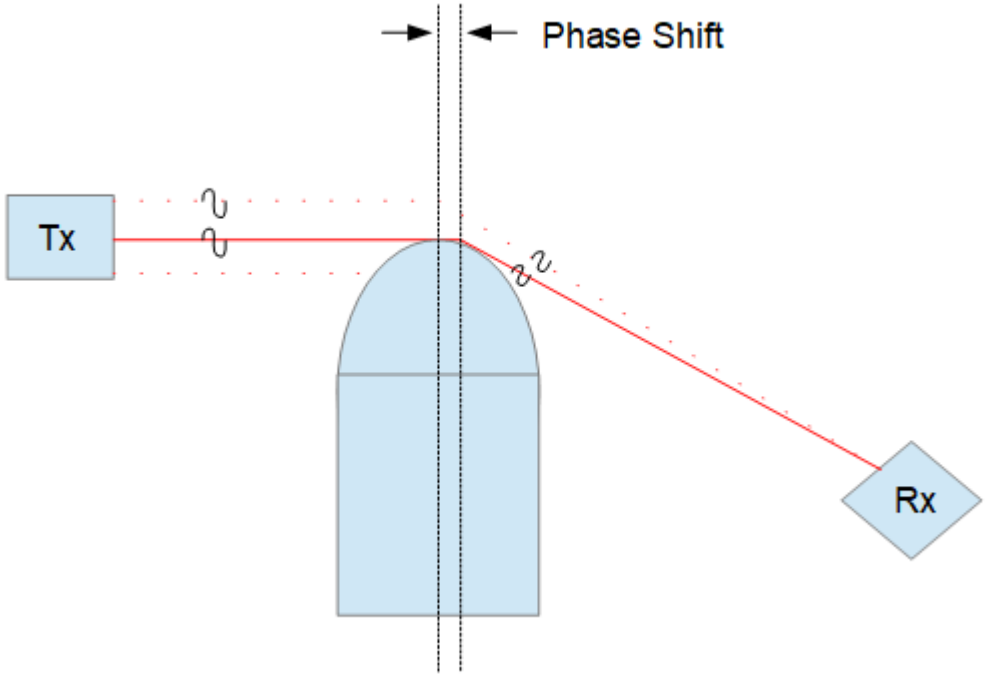

Figure 39: Illustration of phase shift between obstructed and unobstructed paths

Speaking in general terms we observed the estimations given in the previous chapter. We observed varying degrees of diffraction loss and gain from interference. We also observed excess loss when sampling the knife at larger offset angles.

It is also interesting to note the little variance in the raw data measured with a standard deviation of 0.0134 (Figure 40). Comparing the noise level of the Anago sharpness tester, which is arguably the best sharpness tester on the market we can see markedly improved accuracy.

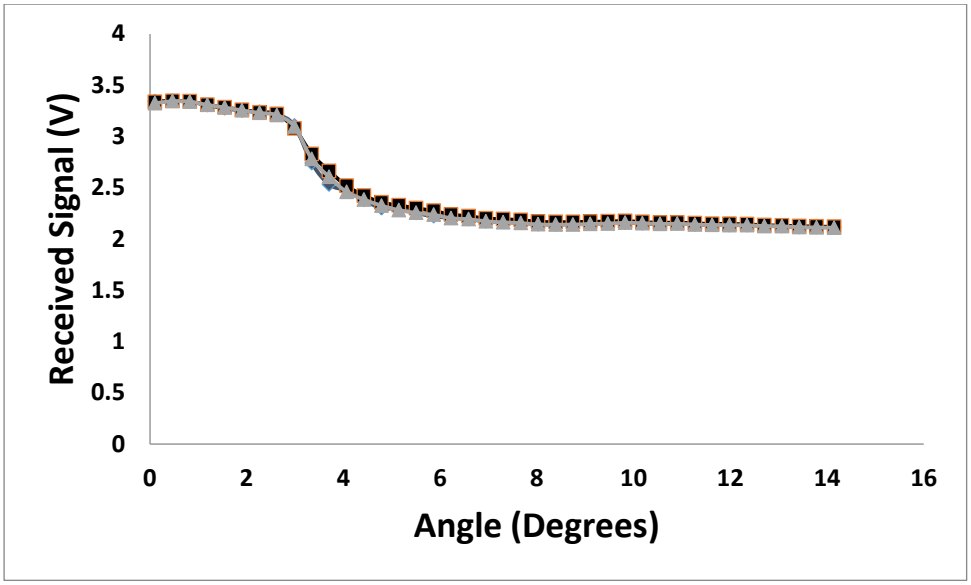

Figure 40: Graph of the raw received data showing very little variance between three tests at the same location. High repeatability

6.2 Verification of Results

In order to verify the results obtained from the prototype, we must review the data given from the Anago knife sharpness tester (KST) and SEM images. The data for knife A, B, and C are respectively presented in Tables 3, 4, and 5. The data is also presented below each table graphically.

Distance (mm)	Anago Score	SEM Diameter (µm)	Prototype Gain/loss (dB)
0	8.8	unclear	6.90
1	8.8	1.74	11.02
2	8.81	unclear	10.49
3	8.83	1.50	11.87
4	8.85	1.73	11.55
5	8.82	1.95	9.54
6	8.8	1.00	13.33
7	8.81	2.20	8.85
8	8.81	3.50	5.27
9	8.81	4.35	3.15

Table 3: Data comparison between the Anago KST, SEM images and prototype measurement for sample A (KST 8.5)

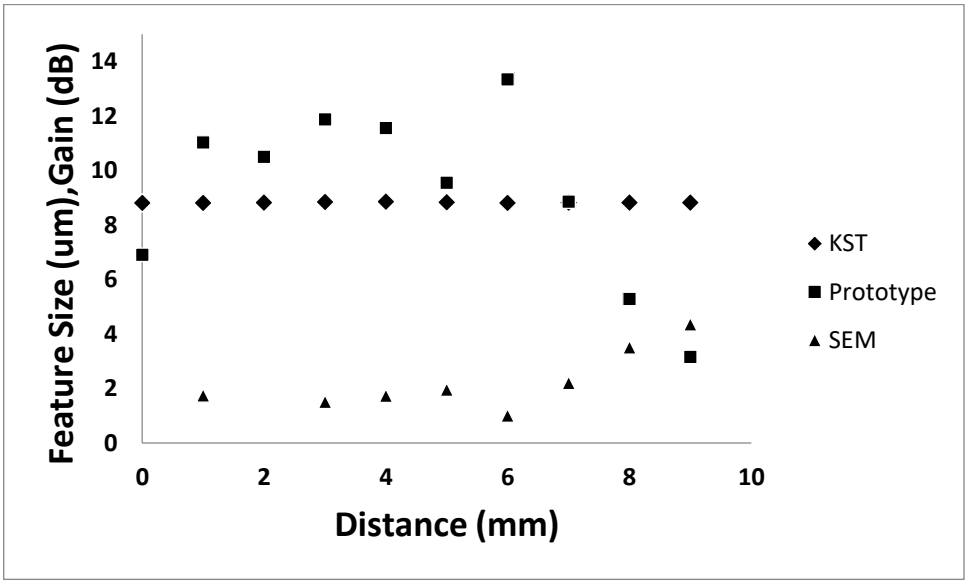

Figure 41 – Comparison for sample A.

Distance (mm)	Anago Score	SEM Radius (µm)	Prototype Gain/loss (dB)
0	6.3	18.00	-1.31
1	6.3	23.50	-7.04
2	6.3	19.20	-2.91
3	6.4	25.00	-7.74
4	6.4	unclear	-7.27
5	6.4	23.00	-5.48
6	6.4	19.00	-3.49
7	6.4	22.20	-4.09
8	6.5	20.00	-5.26
9	6.5	unclear	-6.02

Table 4: Data comparison between the Anago KST, SEM images and prototype measurement for sample B (6.5)

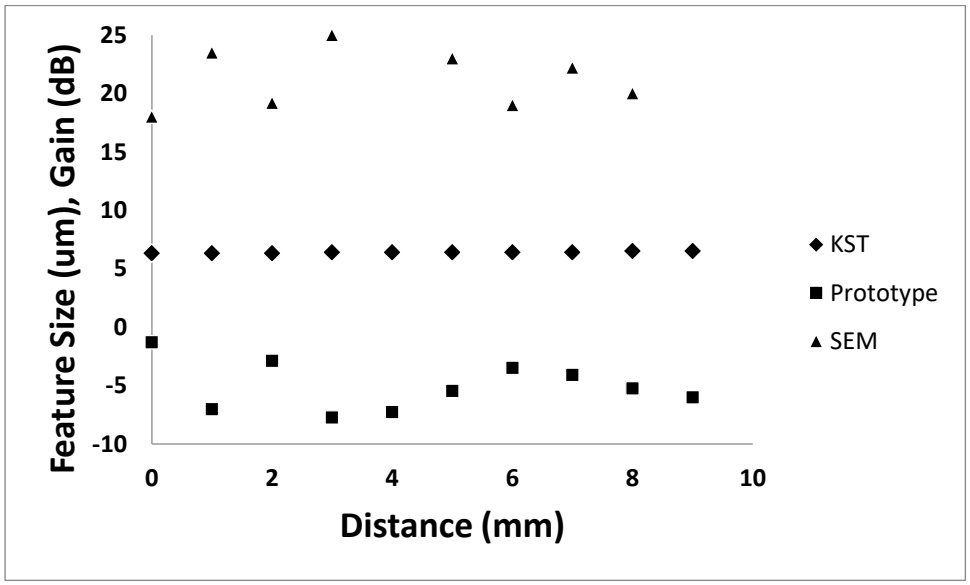

Figure 42 - Comparison for sample B.

Distance (mm)	Anago Score	SEM Radius (µm)	Prototype Gain/loss (dB)
0	5.7	34.00	-28.56
1	5.7	5.20	1.56
2	5.7	10.40	-5.08
3	5.7	30.00	-18.8
4	5.3	13.00	-9.68
5	5.2	20.90	-2.94
6	5.2	13.90	-3.56
7	5.1	unclear	-35.36
8	5.0	29.10	-17.65
9	5.0	unclear	-12.48

Table 5: Data comparison between the Anago KST, SEM images and prototype measurement for sample C (KST 5.5)

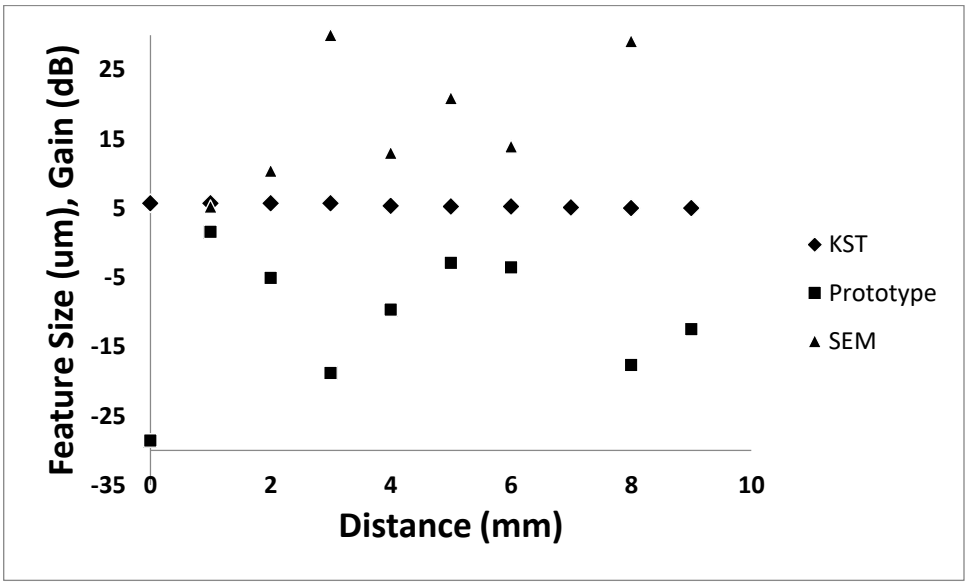

Figure 43 - Comparison for sample C.

It was difficult to compare the SEM and prototype data to the Anago device as the small variations are not apparent in the final score out of ten. This could be in part due to the algorithm used or the mesh target material.

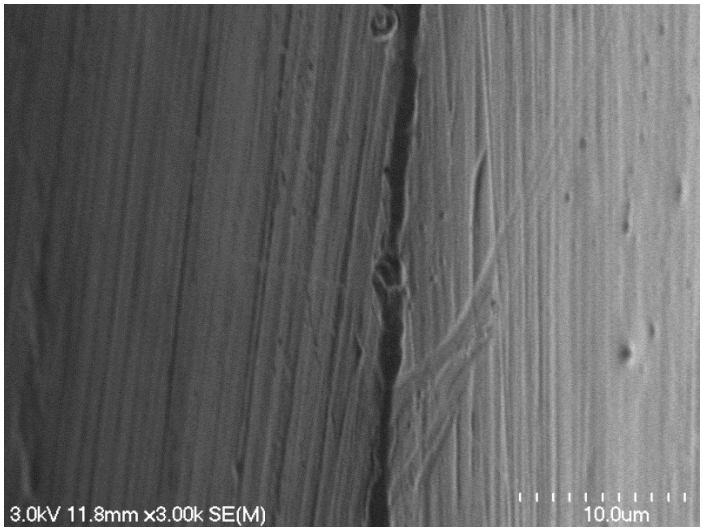

Figure 44: SEM photograph showing the scale that can be observed at a given point

Chapter 7 - Conclusions and Proposals for Future Work

In conclusion, in this work we have developed a testing technique using knife edge diffraction to quantify the sharpness of blades. The results positively conclude that sharpness can be measured by measuring the intensity of diffracted light in the shadowed region of the knife. From the data presented herein we may conclude that this technique has been successfully validated and the results are repeatable. However, to gain further reassurance, future work could include developing a more suitable receiver so that the measurements are more reliable. The receiver appears to clip the upper signal values above that of 3 Volts. This is an issue because sharper knives will have higher gains than those that are dull, but that cannot not be seen because of the clipping. The effects of diffraction could be measured closer to the grazing point if we could remove the clipping and therefore simplify the process of the measurement.

Future work could also include a better method to correlate the physical radius of a cutting edge to the diffracted results measured. It is critical to completely validate this research that more data is collected from SEM images that is more representable of the knife edge and not just a small fraction of it.

In a future iteration of this prototype, I suggest developing a more stable prototype that removes variations in receiver rotation with a capable trans-impedance amplifier to eliminate the low level saturation found in the current prototype. Once these issues have been cleared up, Equation 5.10 may be used to deduce the radius of a knife edge using the excess loss measured from the system.

Through-out this work, we classify sharpness and what a knife failure mode looks like. From there we have been able to positively identify the leading cause of dull knives used in industry.

Following this work, a manuscript will be prepared for publication for the IEEE *Transactions* on Instrumentation and Measurement journal.

Bibliography

[1] Anago. (2018). Anago | Ensure Optimum Sharpness and Improve Productivity. Retrieved from http://anago.co.nz/

[2] Anderson, T. (2005). Fracture Mechanics (3rd ed., pp. 14-40). Florida: CRC Press.

[3] Blade Forums. (2018). Insane performance boost in cutting ability!. Retrieved from https://www.bladeforums.com/threads/insane-performance-boost-in-cutting-ability.1257278/page-2

[4] Brubacher, M. (2018). Index. Retrieved from http://www.edgeonup.com/index.html

[5] CATRA Life Tester. (2018). Sharpness life tester. Retrieved from http://www.catra.org/pages/products/kniveslevel1/slt.htm

[6] CATRA Sharpness Tester. (2018). Sharpness tester. Retrieved from http://www.catra.org/pages/products/kniveslevel1/st.htm [6] Gabriella, & Samantha. (2018). The Definitive Guide to Knife Edges - The Kitchen Professor. Retrieved from https://thekitchenprofessor.com/blog/a-guide-to-knife-edges

[7] Edge on up. (2018). Index. Retrieved from http://edgeonup.com/

[8] Fan, Y., & Du, R. (1996). Monitoring Rotating Tools Using Laser Diffraction. Journal Of Manufacturing Science And Engineering, 118(4), 664. doi: 10.1115/1.2831083

[9] Gabriella, & Samantha. (2018). The Definitive Guide to Knife Edges - The Kitchen Professor. Retrieved from https://thekitchenprofessor.com/blog/a-guide-to-knife-edges

[10] Green, A., & Legato, S. The butcher's apprentice (pp. 10-11).

[11] Hacking, K. (1970). U.H.F. propagation over rounded hills. Proceedings Of The Institution Of Electrical Engineers, 117(3), 499. doi: 10.1049/piee.1970.0101

[12] Haida. (2018). Knives Sharpness Test Equipment - Cookware Testing Equipment. Retrieved from http://www.haidatestequipment.com/products/knives-sharpness-test-equipment.htm [10] Phillipson, D. (2005). African Archaeology (3rd ed., pp. 54-55). New York: Cambridge University Press.

[13] Hodges, D., & Toivonen, P. (2008). Quality of fresh-cut fruits and vegetables as affected by exposure to abiotic stress. Postharvest Biology And Technology, 48(2), 155-162. doi: 10.1016/j.postharvbio.2007.10.016

[14] Jeon, S., Stepanick, C., Zolfaghari, A., & Lee, C. (2017). Knife-edge interferometry for cutting tool wear monitoring. Precision Engineering, 50, 354-360. doi: 10.1016/j.precisioneng.2017.06.009 [13] McCarthy, C., Hussey, M., & Gilchrist, M. (2007). On the sharpness of straight edge blades in cutting soft solids: Part I – indentation experiments. Engineering Fracture Mechanics, 74(14), 2205-2224. doi: 10.1016/j.engfracmech.2006.10.015

[15] Komanduri, R., Chandrasekaran, N., & Raff, L. (1998). Effect of tool geometry in nanometric cutting: a molecular dynamics simulation approach. Wear, 219(1), 84-97. doi: 10.1016/s0043-1648(98)00229-4

[16] Lebeau, R. (2003). Optical sharpness meter. United States of America.

[17] Lee, C., Mahajan, S., Zhao, R., & Jeon, S. (2016). A curved edge diffraction-utilized displacement sensor for spindle metrology. Review Of Scientific Instruments, 87(7), 075113. doi: 10.1063/1.4958882

[18] Lindsay, J. (2008). Daily life in the medieval Islamic world (p. 64). Indianapolis, Ind.: Hackett.

[19] Mach, K., Nelson, D., & Denny, M. (2007). Techniques for predicting the lifetimes of wave-swept macroalgae: a primer on fracture mechanics and crack growth. Journal Of Experimental Biology, 210(13), 2213-2230. doi: 10.1242/jeb.001560

[20] Mandeville, J. (2018). Sharpening a Survival Knife. Retrieved from http://www.survival-expert.com/sharpening_knives.htm

[21] McCarthy, C., Annaidh, A., & Gilchrist, M. (2010). On the sharpness of straight edge blades in cutting soft solids: Part II – Analysis of blade geometry. Engineering Fracture Mechanics, 77(3), 437-451. doi: 10.1016/j.engfracmech.2009.10.003

[22] McCarthy, C., Hussey, M., & Gilchrist, M. (2007). On the sharpness of straight edge blades in cutting soft solids: Part I – indentation experiments. Engineering Fracture Mechanics, 74(14), 2205-2224. doi: 10.1016/j.engfracmech.2006.10.015

[23] McGinty, B. (2018). LEFM. Retrieved from http://www.fracturemechanics.org/LEFM.html

[24] McGorry, R., Dowd, P., & Dempsey, P. (2005). A technique for field measurement of knife sharpness. Applied Ergonomics, 36(5), 635-640. doi: 10.1016/j.apergo.2005.04.001

[25] McGorry, R., Dowd, P., & Dempsey, P. (2003). Cutting moments and grip forces in meat cutting operations and the effect of knife sharpness. Applied Ergonomics, 34(4), 375-382. doi: 10.1016/s0003-6870(03)00041-3

[26] McLarnon, B. (1997). VHF/UHF/Microwave Radio Propagation: A Primer for Digital Experimenters. Retrieved from https://www.tapr.org/ve3jf.dcc97.html

[27] Mishra, P. (2016). Stress Strain Curve – Relationship, Diagram and Explanation. Retrieved from http://www.mechanicalbooster.com/2016/09/stress-strain-curve-relationship-diagram-explanation.html

[28] NSF. (2018). What Is NSF Certification? - NSF International. Retrieved from http://www.nsf.org/consumer-resources/what-is-nsf-certification

[29] Ochsner, J., Cooley, D., & LeMaire, S. (2009). Surgical Knife. Texas Heart Institute, 36(5), 441-443. Retrieved from https://www.ncbi.nlm.nih.gov/pmc/articles/PMC2763477/

[30] Palmer, G. (2018). What Is Pakkawood? | Hunker. Retrieved from https://www.hunker.com/12003642/what-is-pakkawood

[31] Phillipson, D. (2005). African Archaeology (3rd ed., pp. 54-55). New York: Cambridge University Press.

[32] Schuldt, S., Arnold, G., Kowalewski, J., Schneider, Y., & Rohm, H. (2016). Analysis of the sharpness of blades for food cutting. Journal Of Food Engineering, 188, 13-20. doi: 10.1016/j.jfoodeng.2016.04.022

[33] Sharpening Supplies. (2018). Detailed Discussion on Knife Sharpening Angles. Retrieved from https://www.sharpeningsupplies.com/Detailed-Discussion-on-Knife-Sharpening-Angles-W28.aspx

[34] Tappin, D., Bentley, T., & Vitalis, A. (2008). The role of contextual factors for musculoskeletal disorders in the New Zealand meat processing industry. Ergonomics, 51(10), 1576-1593. doi: 10.1080/00140130802238630

[35] Thacker, J., Rodeheaver, G., Towler, M., & Edlich, R. (1989). Surgical needle sharpness. The American Journal Of Surgery, 157(3), 334-339. doi: 10.1016/0002-9610(89)90565-5

[36] TORMEK. (2018). TORMEK - Knife Jig | Tools4Wood. Retrieved from https://www.tools4wood.co.za/product/tormek-knife-jig-svm-45/

[37] Watkins, F., London, S., Neal, J., Thacker, J., & Edlich, R. (1997). Biomechanical performance of cutting edge surgical needles. The Journal Of Emergency Medicine, 15(5), 679-685. doi: 10.1016/s0736-4679(97)00149-2

[38] WebstaurantStore. (2018). Types of Knives. Retrieved from https://www.webstaurantstore.com/guide/538/types-of-knives.html.

[39] Weon Kim, K., Young Lee, W., & Chol Sin, H. (1999). A finite-element analysis of machining with the tool edge considered. Journal Of Materials Processing Technology, 86(1-3), 45-55. doi: 10.1016/s0924-0136(98)00230-1

[40] Willis, M. (2018). Propagation Tutorial - Diffraction. Retrieved from http://www.mike-willis.com/Tutorial/PF7.htm

[41] Wireless System Design. (2013). Fresnel Zones and Diffraction. Lecture, The University of British Columbia.